Sandia National Laboratories

SAND2020-1380PE

From Glass Ceramics to Batteries: Understanding Harder Soft Matter

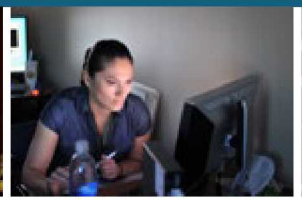

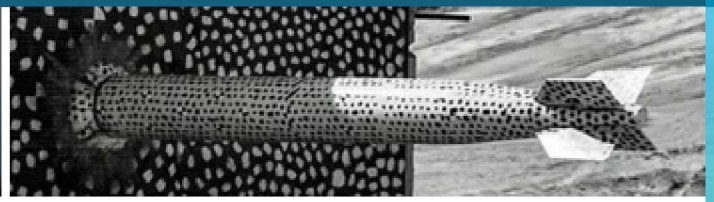

PRESENTED BY

Anne M. Grillet

Engineering Sciences Division

Sandia National Laboratories is a multimission laboratory managed and operated by National Technology and Engineering Solutions of Sandia LLC, a wholly owned subsidiary of Honeywell International Inc. for the U.S. Department of Energy's National Nuclear Security Administration under contract DE-NA0003525.

Sandia National Laboratories

Sandia provides the science needed to enable the U.S. nuclear stockpile, and does fundamental scientific, biomedical, and environmental research to enhance national security, economic competitiveness, and improved quality of life.

Nuclear Deterrence

Defense Nuclear Nonproliferation

National Security Programs

Energy & Homeland Security

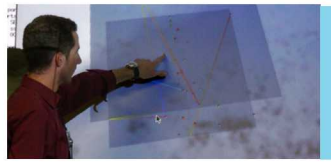

Advanced Science & Technology

"Exceptional Service in the National Interest"

Detection of IEDs through improved radar
Contingency plans for aircraft attacks on critical facilities after 9/11
Deepwater Horizon well capping
Invention of the clean room
Anthrax detection

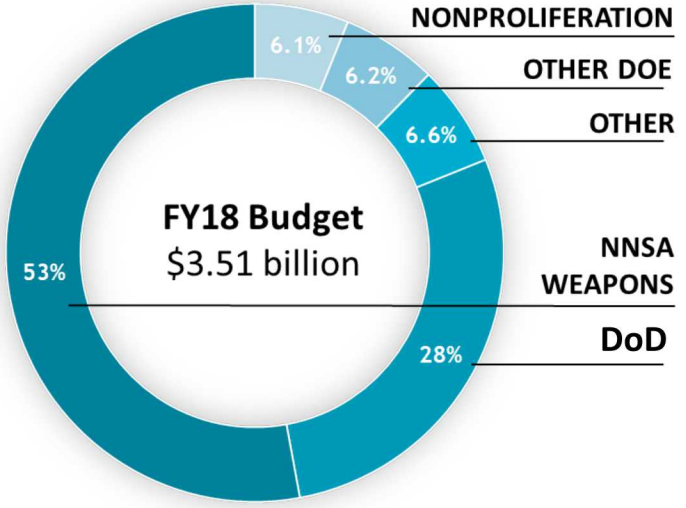

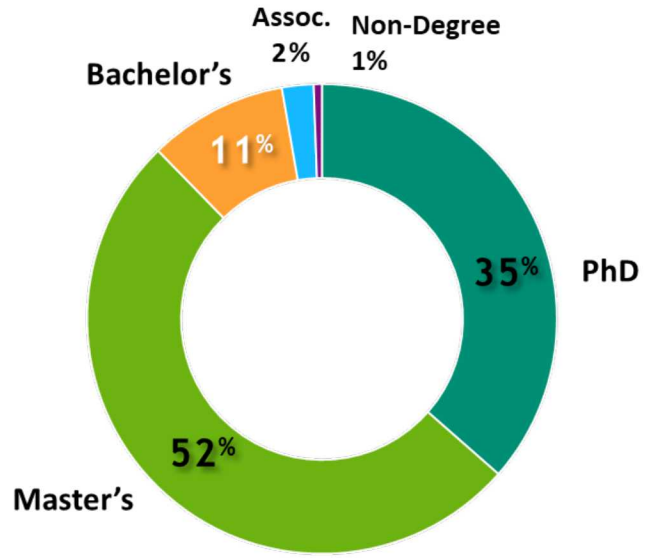

Check out: tours.sandia.gov

SIERRA: HIGHLY COUPLED MULTIPHYSICS FEM CODE

Thermal/mechanical response of salt repository after 27 years of aging

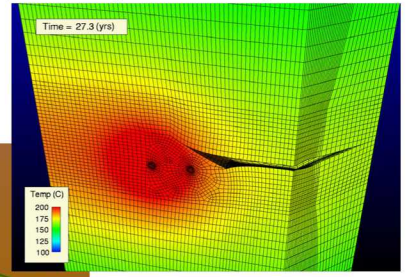

Flight performance: Aero/Mechanical

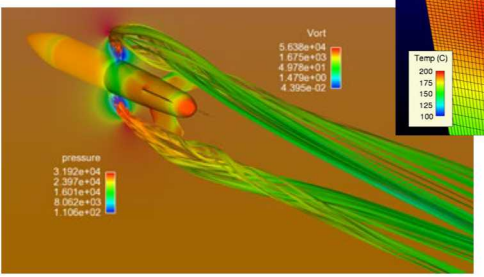

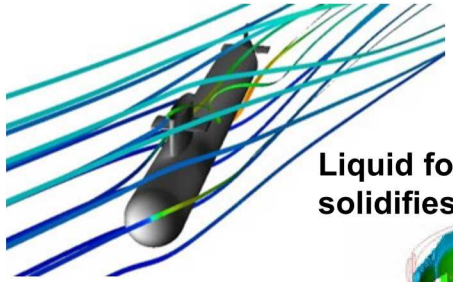

Liquid foam reacts, expands, solidifies to fill a mold

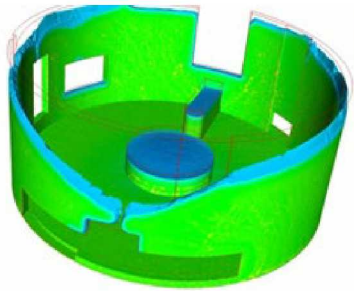

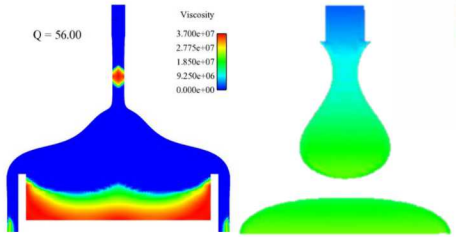

Goma: Open source! Liquid (incompressible) flows, Non-Newtonian

Fire near volume of interest

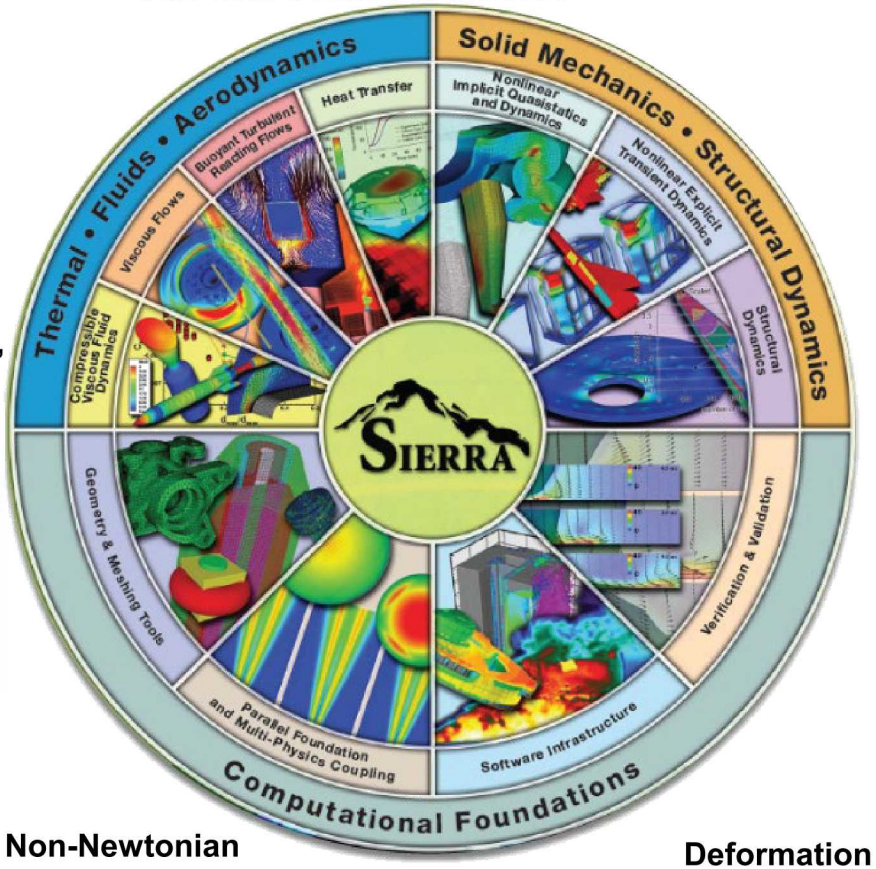

Heat transfer: can include radiation, chemistry

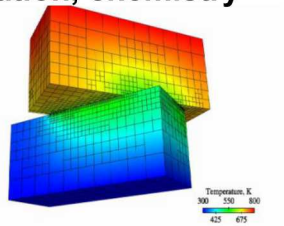

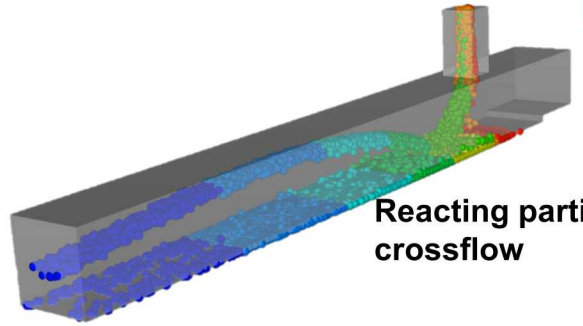

Reacting particles in crossflow

Nalu: Open source! low mach, compressible flows

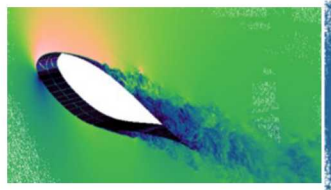

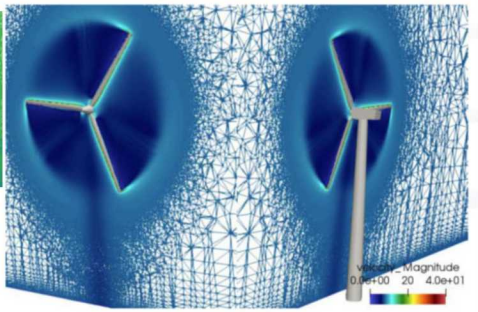

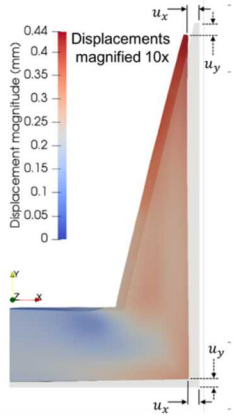

Deformation of solid foam due to aging

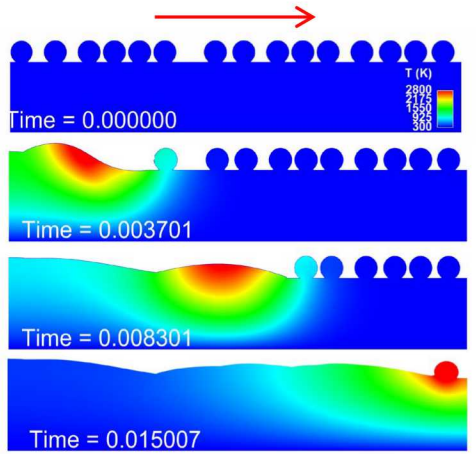

Additive Manufacturing via selective laser melting

Discrete Particle Simulations

LAMMPS

Open Source Molecular Dynamics

Shock loading of polymer foam

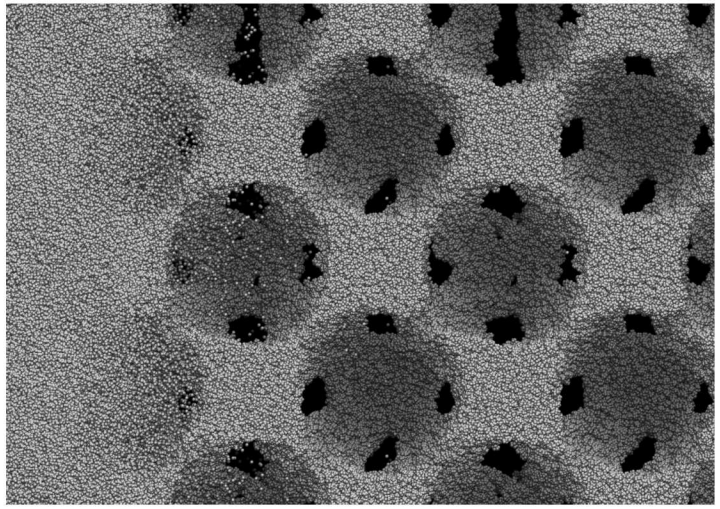

Stress fields around dislocations

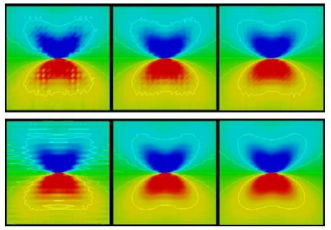

Hot and cold particles in a volume with heat transfer

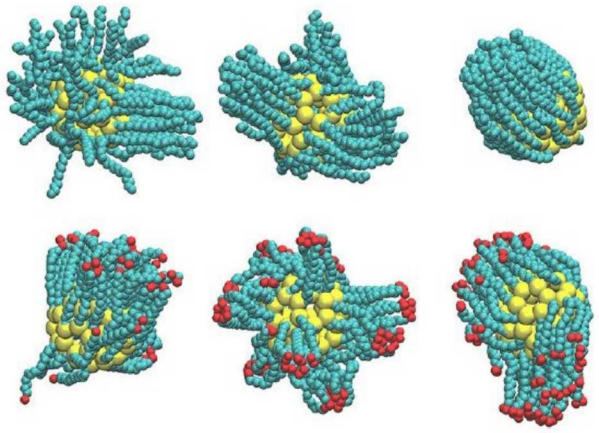

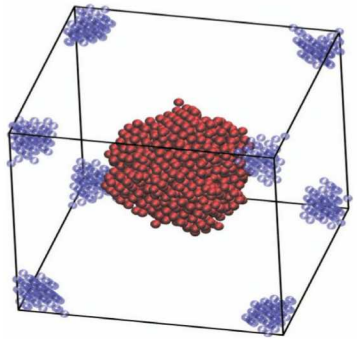

Nanoparticles coated by a polymer in a solvent

ALEPH

Advanced Plasma Transport & Kinetics

Particle in Cell Plasma modeling code

Plasma expansion

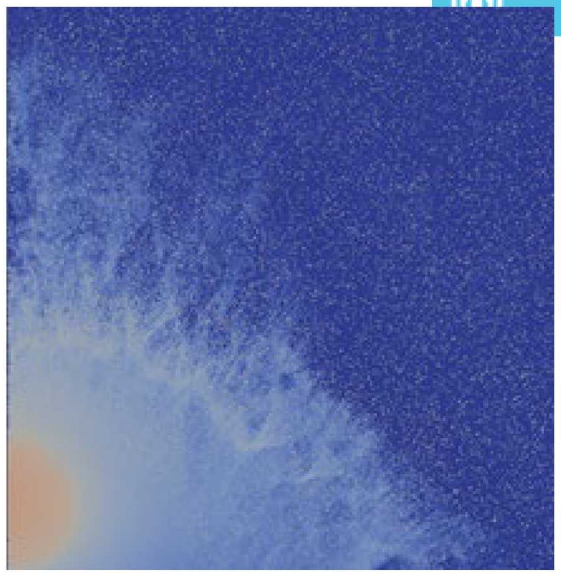

Electrical breakdown in Taylor Anvil

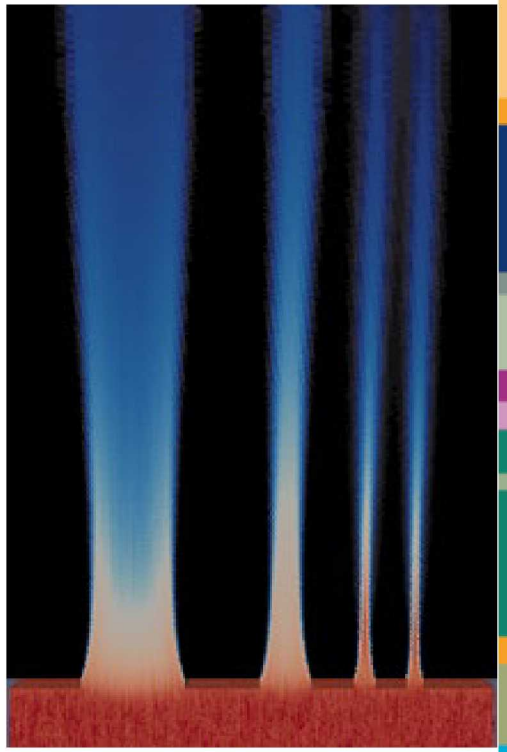

Ion extraction from a plasma

WHAT DOES THE ENGINEERING SCIENCES SOFT MATTER LAB DO?

Rheology and....
- Impedance Measurements (batteries)
- Microscopy (foams)
- Raman spectroscopy (encapsulants)
- High temperature (molten metals)
- Powder flows (batteries)

Low temperature viscosity

Custom diagnostics: Thermal battery visualization

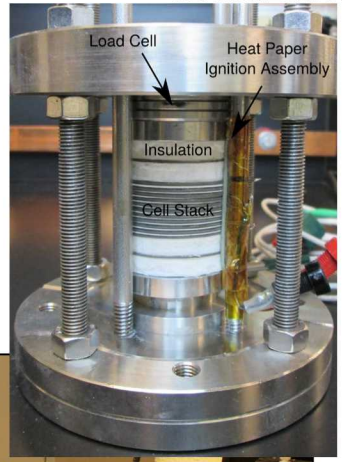

mech properties of partially saturated powders

Micro X-ray CT-- 3µm resolution
Image Analysis

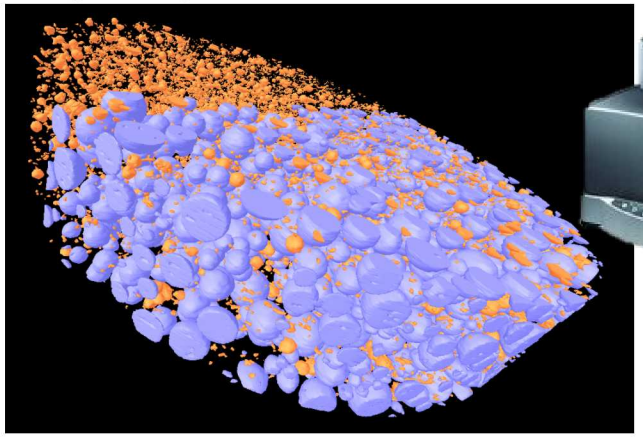

Diffusion through battery

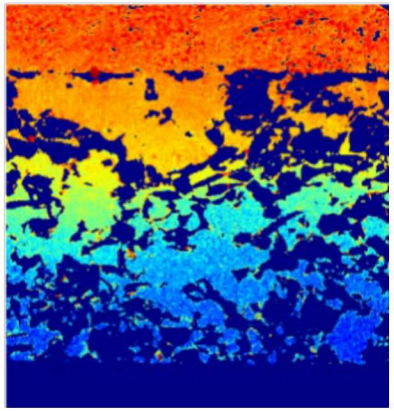

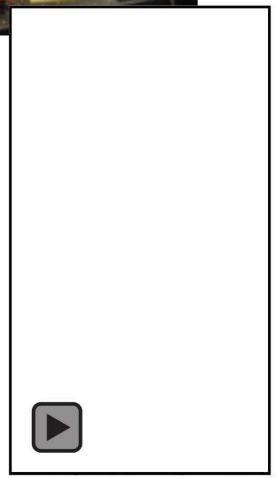

Particle Tracking
High speed camera
Microfluidics

Foam visualization

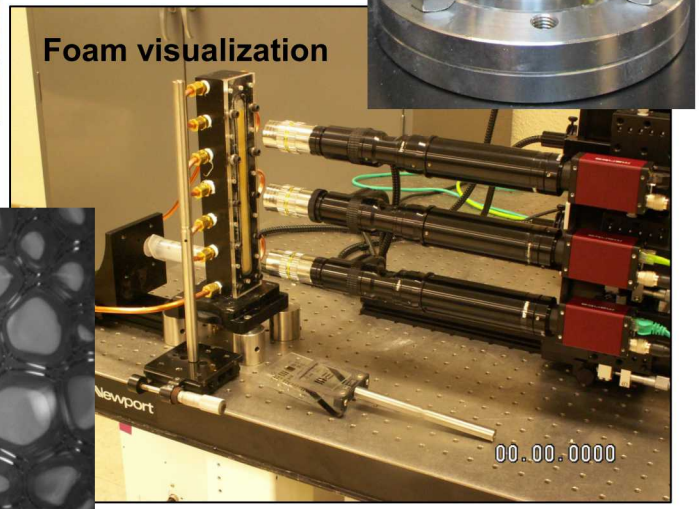

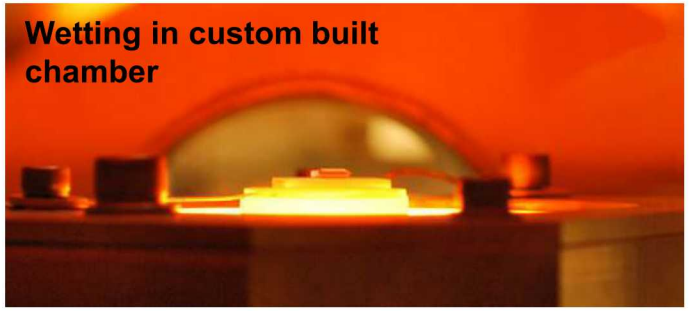

Wetting in custom built chamber

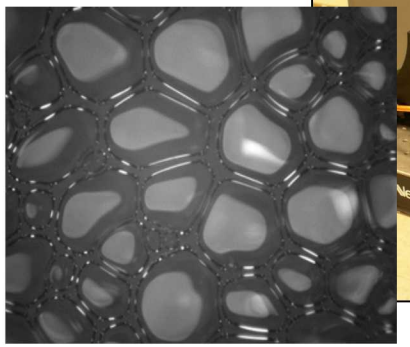

OUTLINE

- Introduction to Sandia
- Glass Ceramics
- Lithium Ion Batteries

Rheology of glass-ceramics for sealing applications

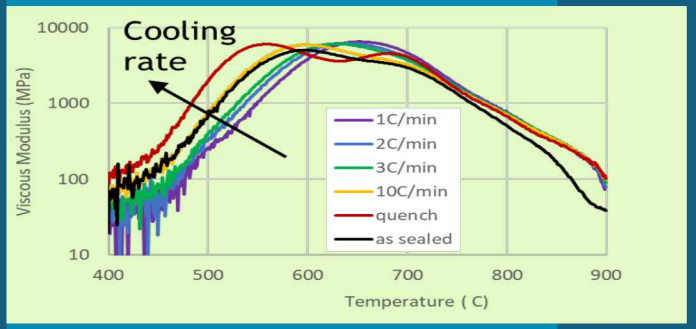

PRESENTED BY

Anne M. Grillet, Steve Dai & Brenton Elisberg

Sandia National Laboratories, P.O. Box 5800
Albuquerque, NM 87185

Sandia National Laboratories is a multimission laboratory managed and operated by National Technology and Engineering Solutions of Sandia LLC, a wholly owned subsidiary of Honeywell International Inc. for the U.S. Department of Energy's National Nuclear Security Administration under contract DE-NA0003525.

Outline

- Introduction to glass and glass ceramic to metal seals
- Modeling needs
- Measurement of shear moduli
- Construction of master curve and calculation of activation energy
- Thermal dependence of microstructure
- Conclusions

What is a hermetic connector?

Barrier to gas/liquid transfer between environments.

- Allow electrical transmission

Designed for extreme conditions

- Thermal
- Pressure
- Shock/vibration

Many applications:

- Satellites, submarine vehicles, medical, telecommunications, etc.

Types of hermetic connectors

- Matched seals
- **Compression seals**

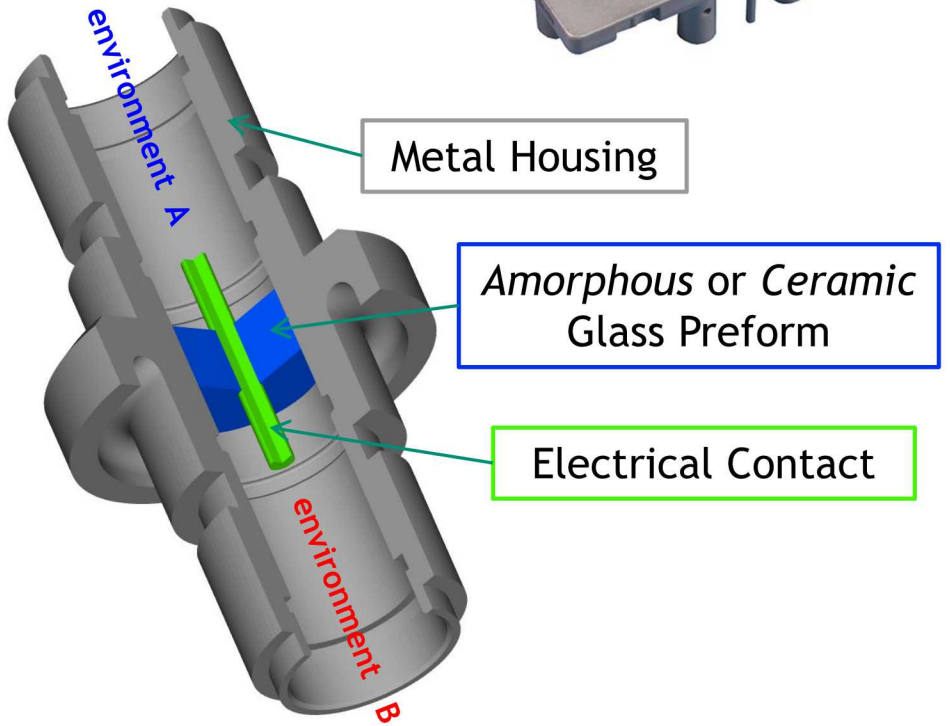

Glass to Metal Seal designs have evolved over the years

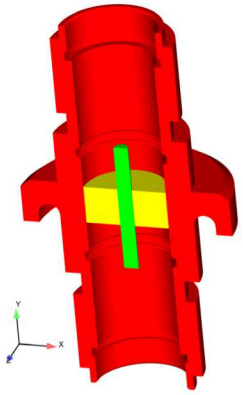

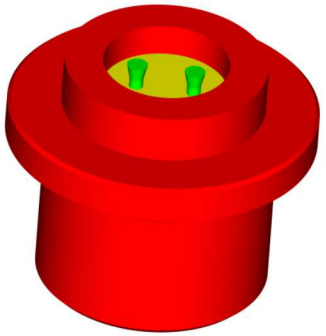

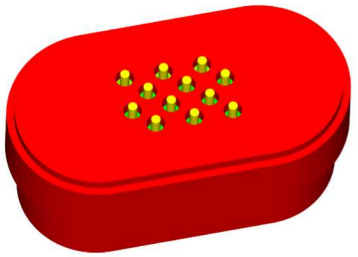

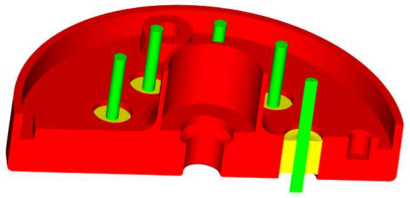

- increasingly complex geometries
- more pins & tighter spacing
- extended life-time requirements
- more complicated materials (e.g., glass ceramics)

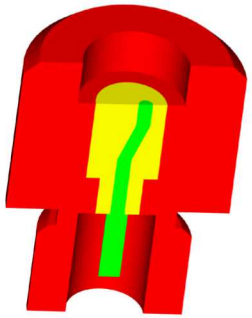

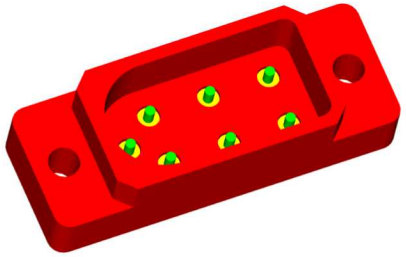

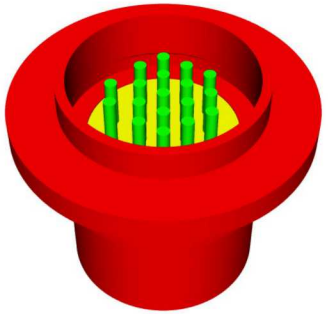

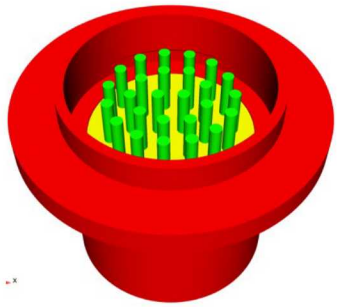

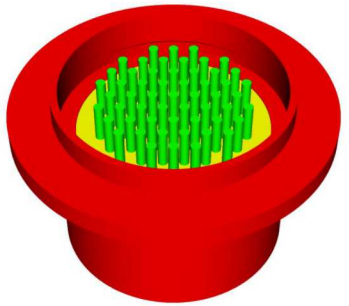

And yet, despite years of experience . . . . . . We still are asking the same questions

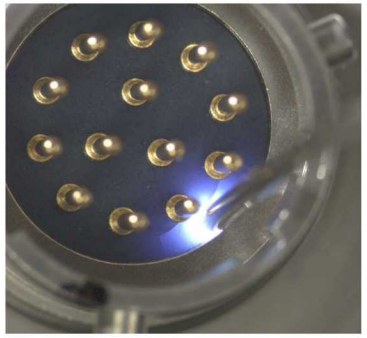

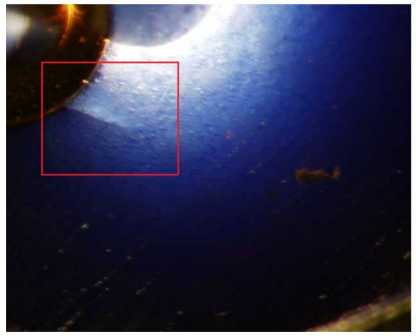

How to design a robust seal?

- Will part remain hermetic?
- Meet life-time requirements?
- Re-use?

Why did the glass crack?

- still hermetic? remain so?
- foreign debris (glass chips)?
- pin stability – short circuits?
- accept or reject parts?

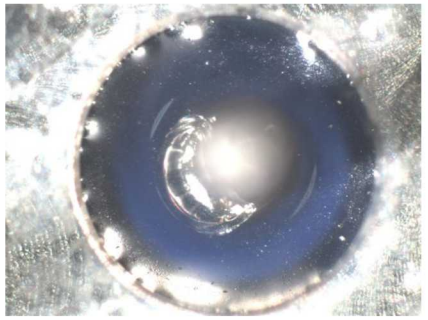

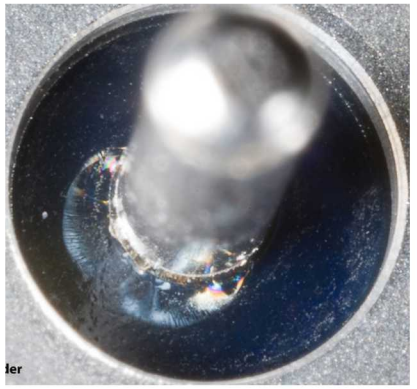

Why Glass-Ceramic to Metal seals?

- Process/reflow like glasses
- High temp stability after crystallization
  - Abnormal high T/P environment
- High coefficient of thermal expansion (CTE)
  - Most sealing glasses < 12 ppm/°C
- Crystallization → tunable coefficient of thermal expansion
- Matched seals:
  - CTE Glass ceramic ≤ CTE housing
- Composite microstructure → toughness/strength

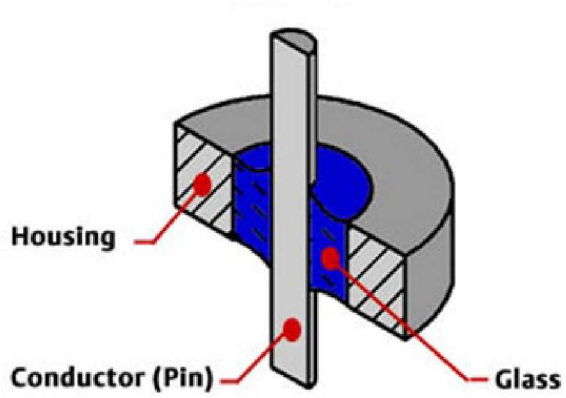

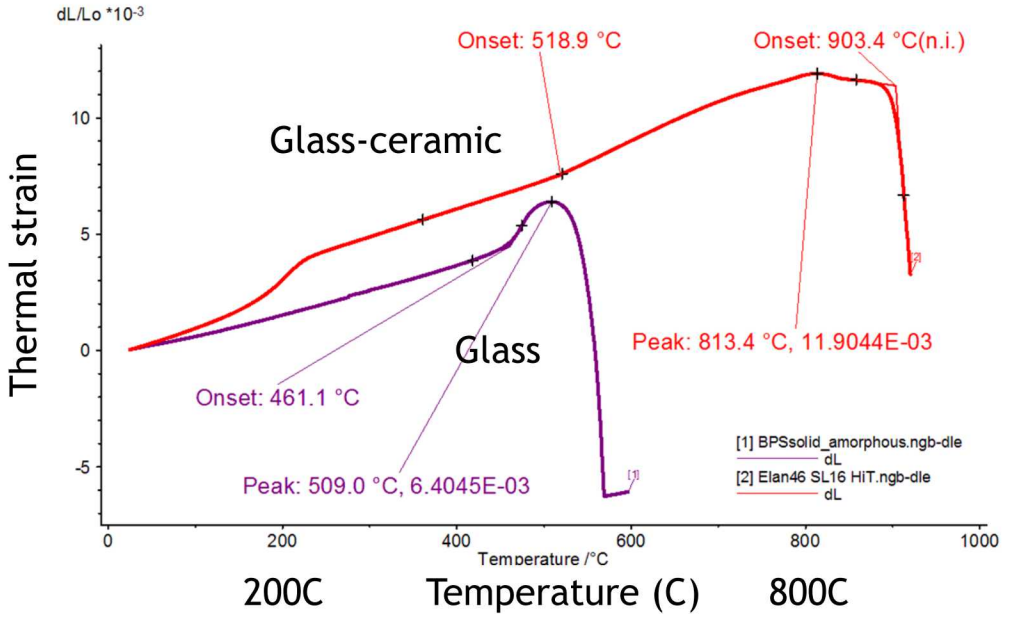

Material	CTE (ppm/°C) (40 -600°C)
304L SS shell	18.89
Glass Ceramic*	16-17
Paliney7 pin	15.76

Sandia Patented Glass Ceramic

Oxide	Wt%
SiO_2	74.3%
B_2O_3	1.2%
Li_2O	12.7%
Al_2O_3	3.8%
K_2O	2.9%
P_2O_5	3.1%
KnO	1.8%

- SiO_2, B_2O_3: Glass network former
- Li_2O, Al_2O_3, K_2O: Glass network modifier
- P_2O_5: → Li_3PO_4 nuclei for crystallization
- KnO: → Corrosion resistance

Phase	CTE (ppm/°C, 40–600°C)
SiO_2, glass	0.5
SiO_2, Quartz	23.3
SiO_2, Cristobalite	27.1
Li_2SiO_3	13.0 (20-300°C)
$Li_2Si_2O_5$	11.0

More cristobalite

Higher CTE

Dai et al. (2016) J. Am Ceramic Soc

Sandia SL16 Glass-ceramics, process and microstructure

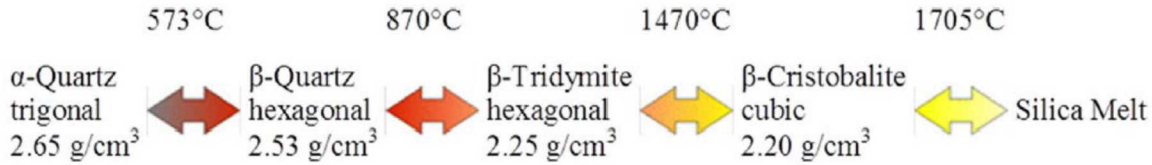

As sealed thermal profile

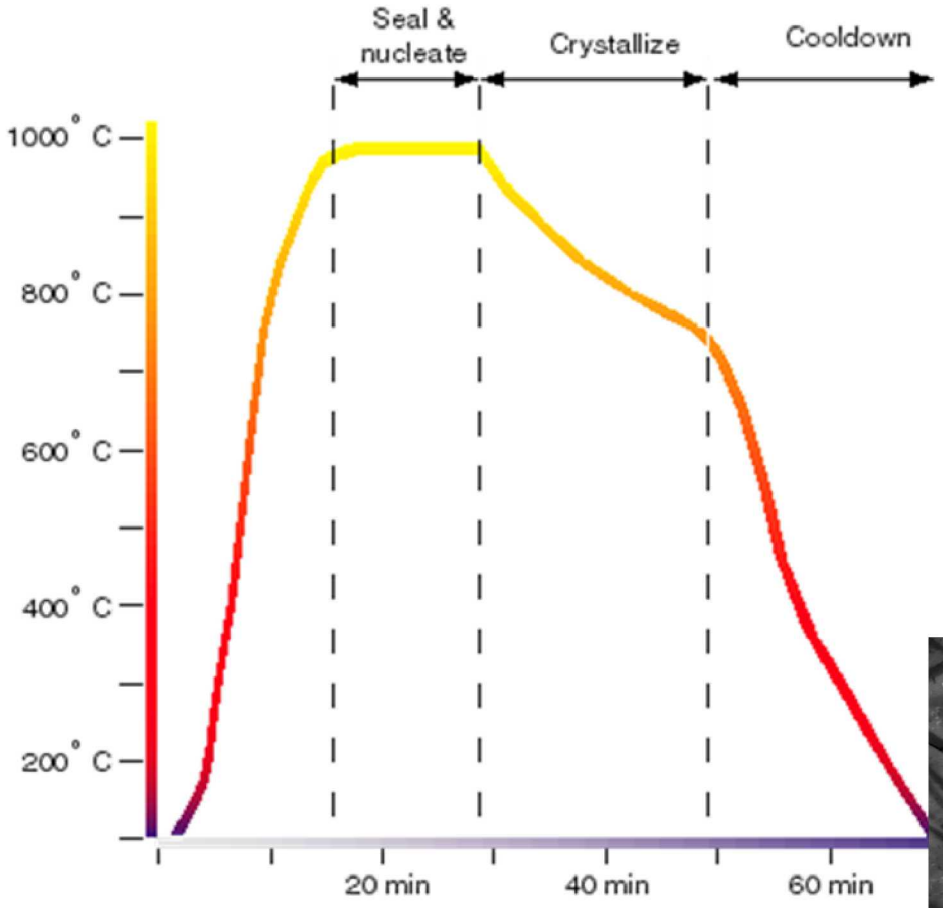

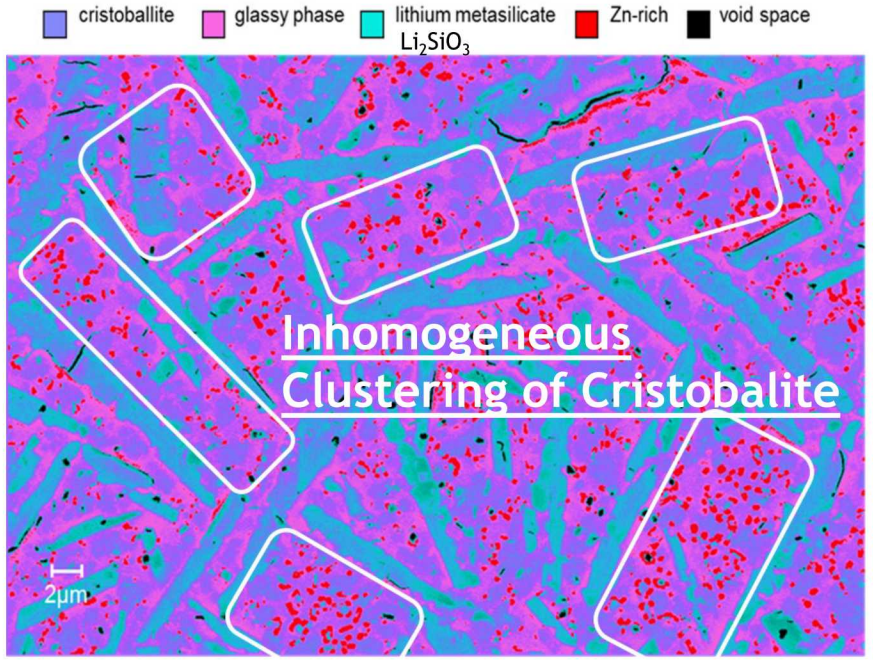

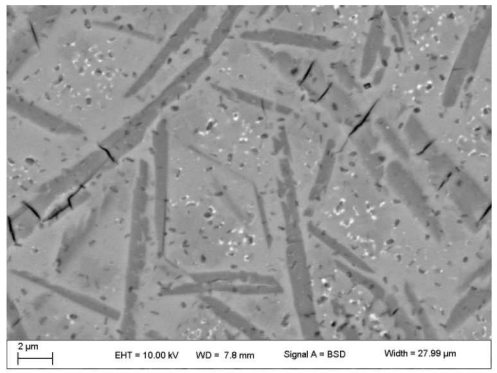

Dai et al. (2016) J. Am Ceramic Soc

Thermal Stress and Strain Prediction

Use Sierra codes to predict stresses and strains after seal processing

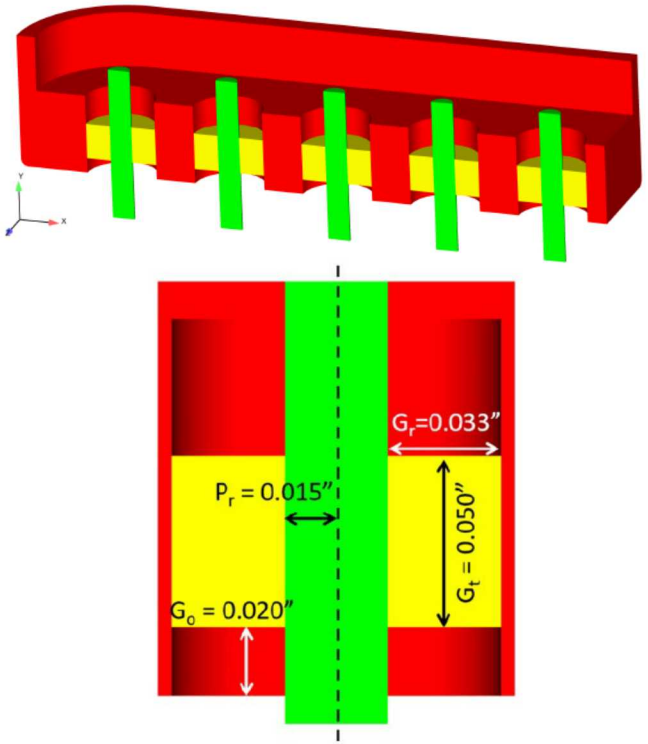

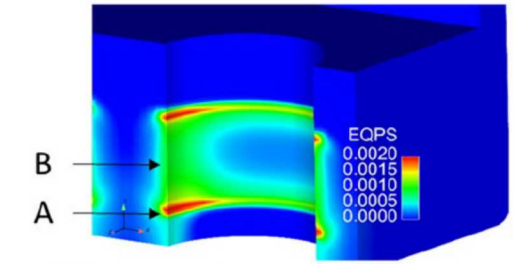

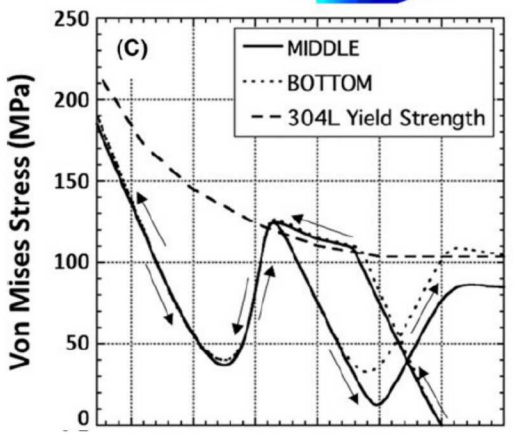

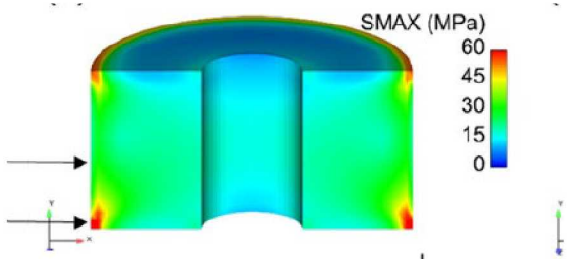

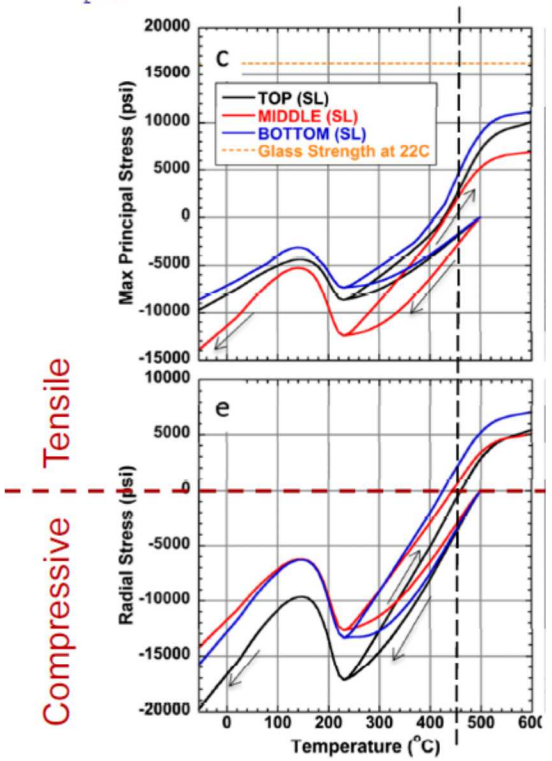

Current predictions are limited to extrapolation of materials properties from 600°C

Dai et al. (2017) J. Am. Ceramic Soc.

Anton Paar:CTD1000 Rheology capability

Rectangular torsion geometry measures shear moduli
Fixtures are made of inconel and they are the only standard ones rated to 1000°C
The stainless steel torsion fixtures are not rated above 600C due to warping
The CTE mismatch doesn't seem to be causing a problem though some slipping with low CTE glasses

Specifications: sample SRF	
Width of sample	1 mm to 12 mm
Thickness of sample	1 mm to 12 mm
Length of sample	**max. 40 mm**

Glass Moduli Temperature Dependence

CABAL 12 is a traditional sealing glass $20MgO\text{-}20CaO\text{-}20Al_2O_3\text{-}40B_2O_3$

Silica free glass developed for lithium battery applications

Comparison of three manufacturer lots

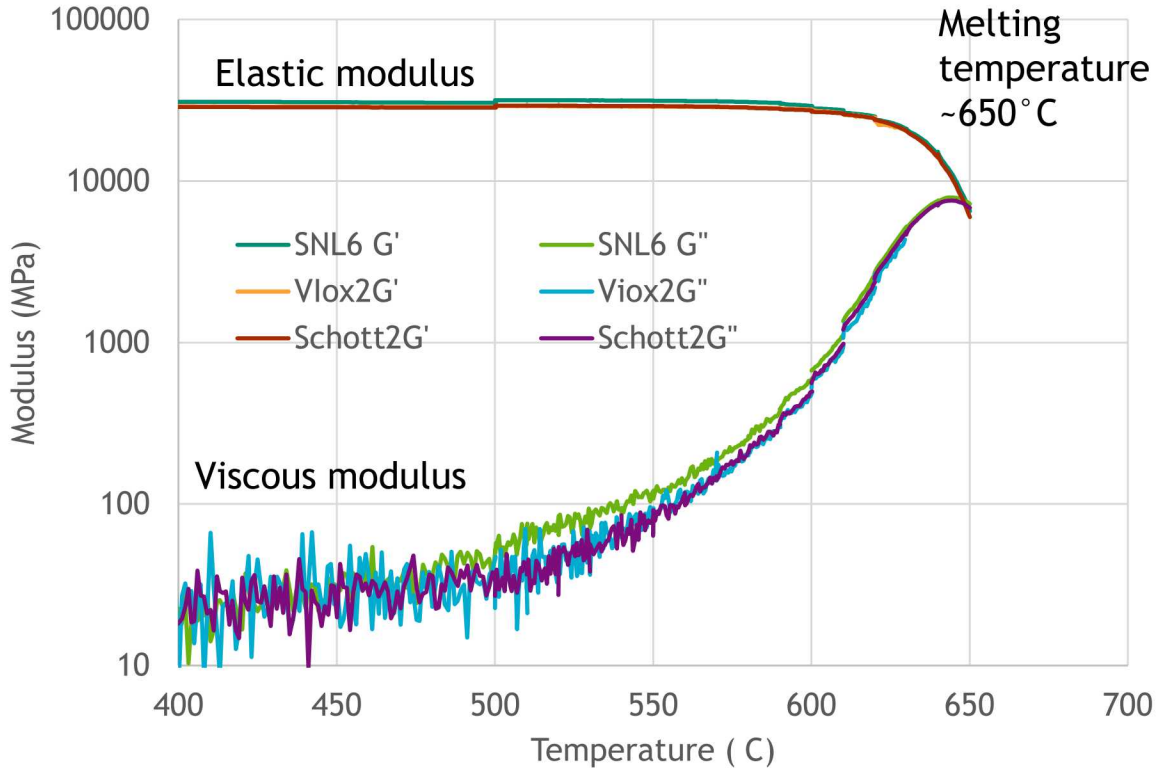

1 Hz, 0.001% strain

Glass-Ceramic Moduli Thermal Dependence

SL 17 composition is Li_2O-SiO_2-Al_2O_3-K_2O-B_2O_3-P_2O_5-ZnO, Ceramed

Annealed 6 /16/16 – 5˚C/min to 700, hold 30min, 1˚C/min to RT

SL derived from step like change in thermal strain caused by cristobalite phase change. 17 refers to CTE ~ 17 ppm/°C

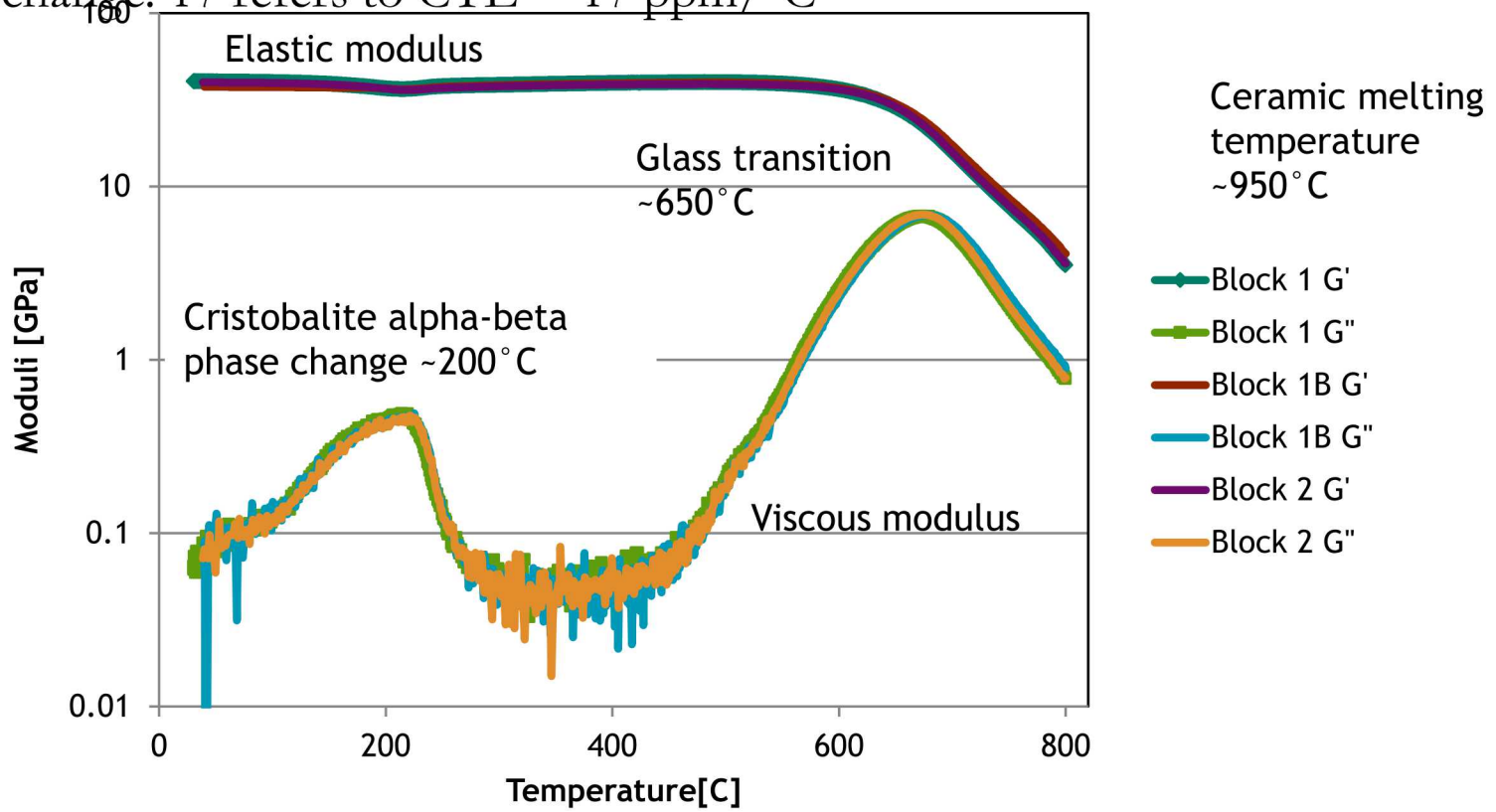

1 Hz, 0.001% strain

Construction of a Master Curve

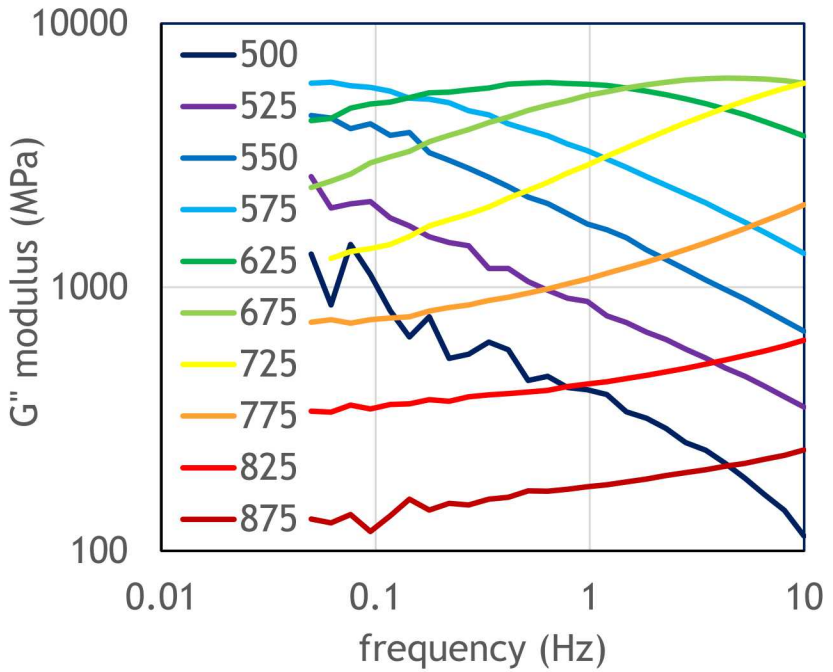

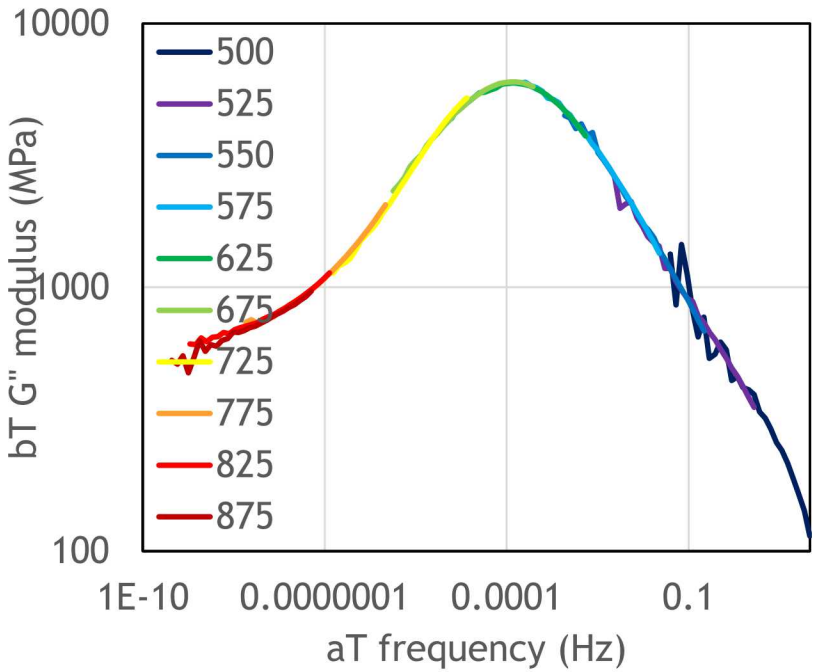

Frequency dependence of viscous modulus as a function of temperature

Apply time temperature superposition to develop a master curve and calculate Arrhenius activation energy

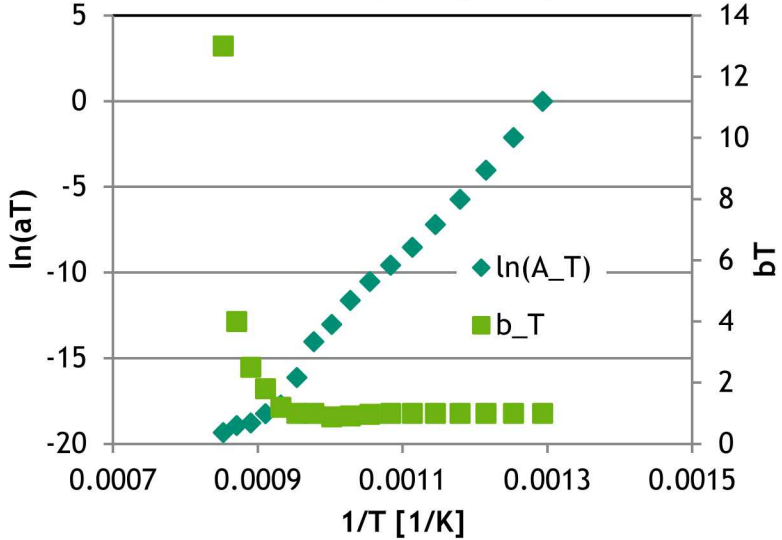

Glass-Ceramic Thermal Dependence

SL16 was ceramed from the same parent crystallizable glass using a different thermal processing, with less high expansion Cristobalite phase, and thus lower CTE ~ 16 ppm/°C.

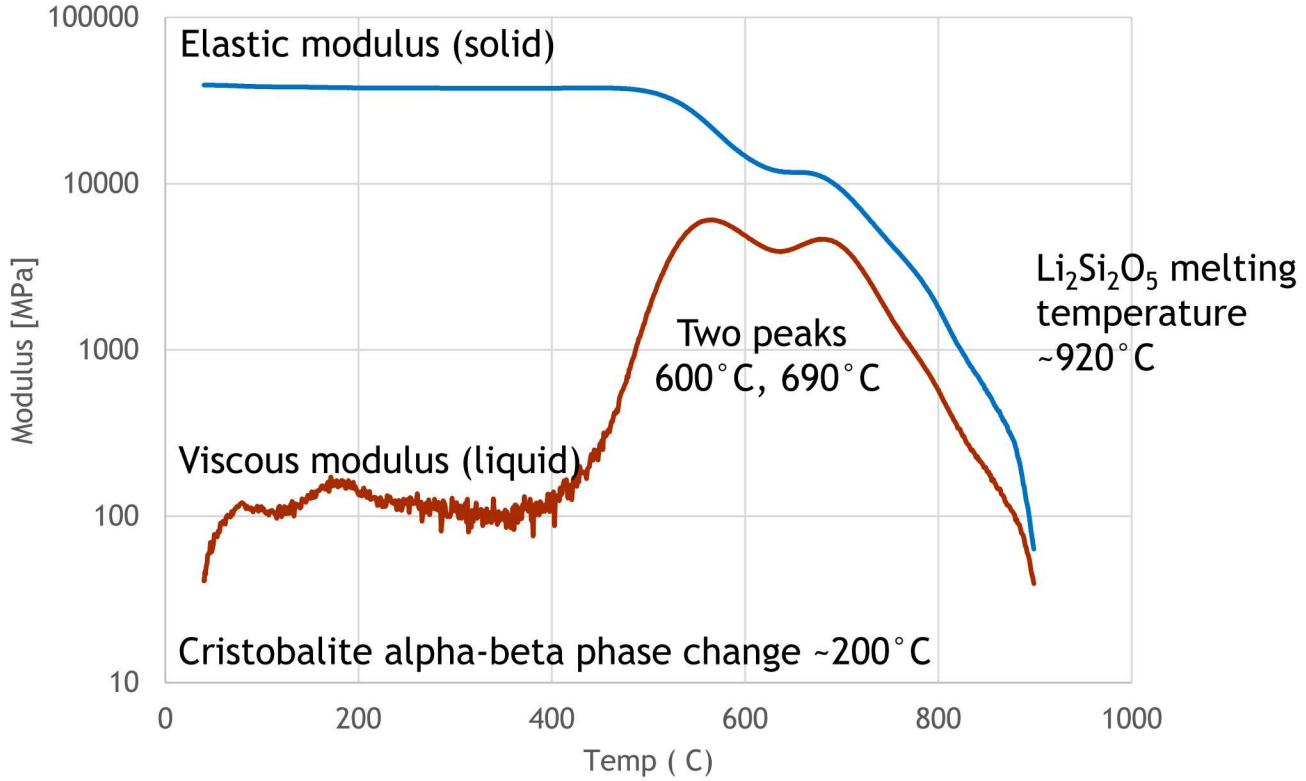

1 Hz, 0.001% strain

Temperature Dependent

See strong dependence in glass transition *during heating* by vary cooling rate from 1°C/min to quenched (decrease ~400°C /10 min)

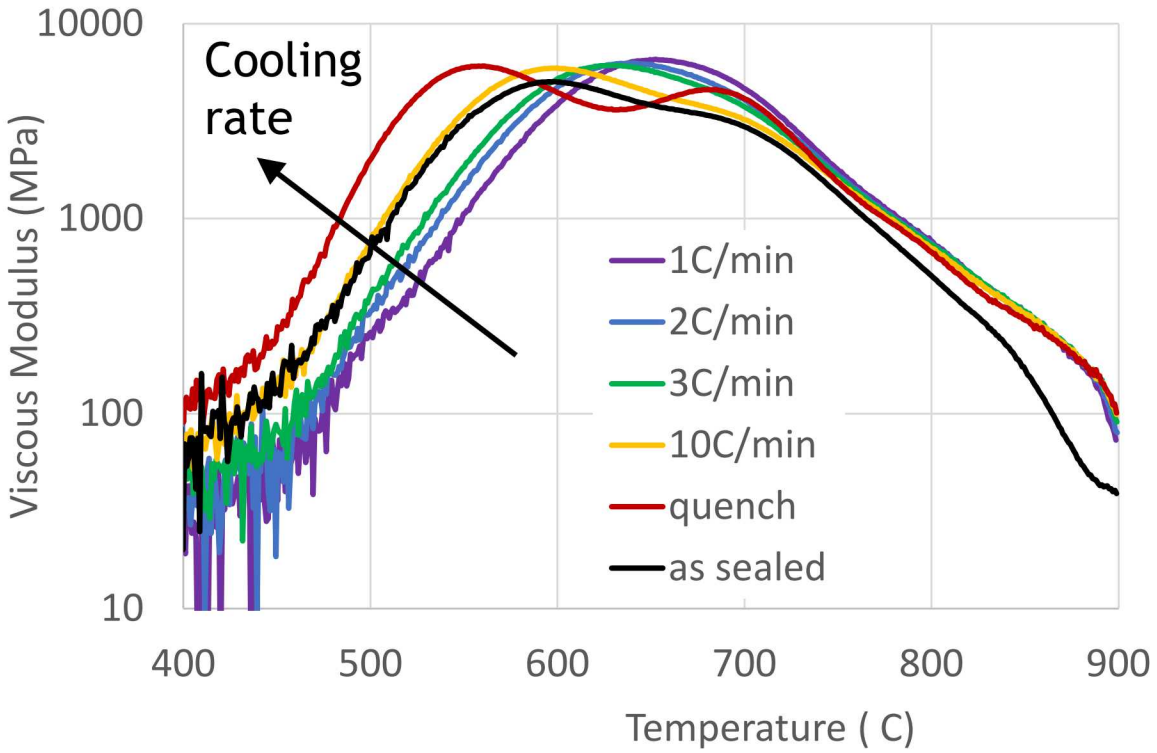

Dynamic restructuring in SL glass ceramics

Time temperature superposition shows evidence of dynamic restructuring of the glass-ceramic well below the melting temperature

Time temperature superposition shows two distinct Arrhenius activation energies,

- Relaxation of residual glass (<600ºC activation energy
- "Re-arrangement" of the crystalline phase, or "configurational" relaxation
- Previous studies found the crystalline composition was stable up to 650ºC

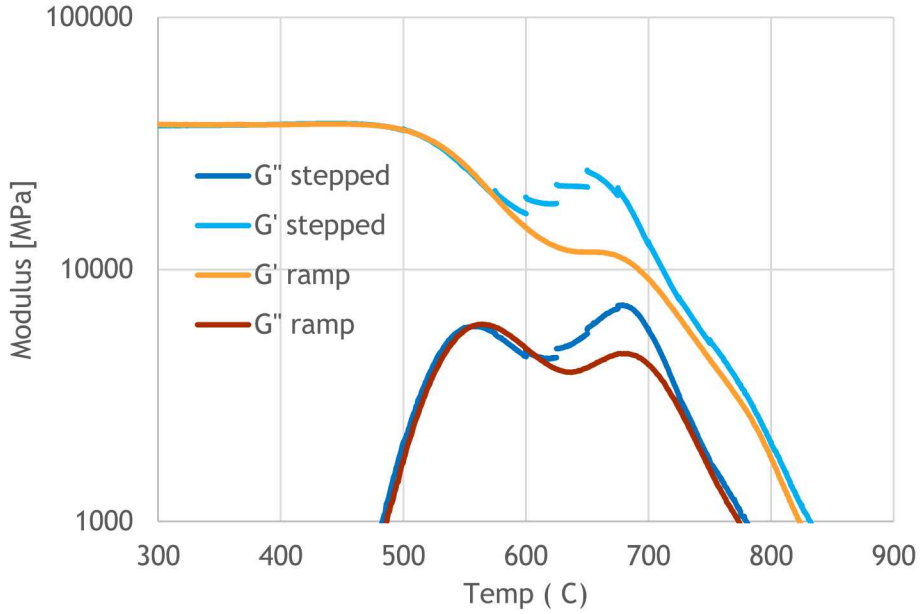

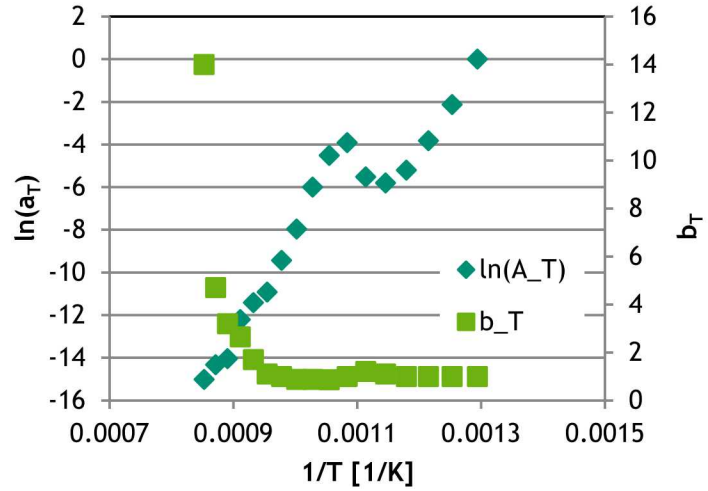

Rodriguez et al. (2016) J. Am Ceram. Soc.

Temperature Dependent Microstructure

Rearrangement is believed to be controlled by diffusion through viscous glassy phase

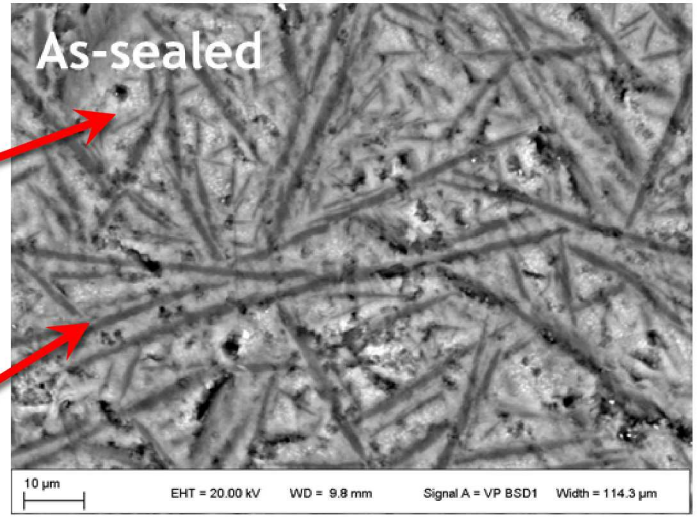

SiO_{2CR}

Li_2SiO_3

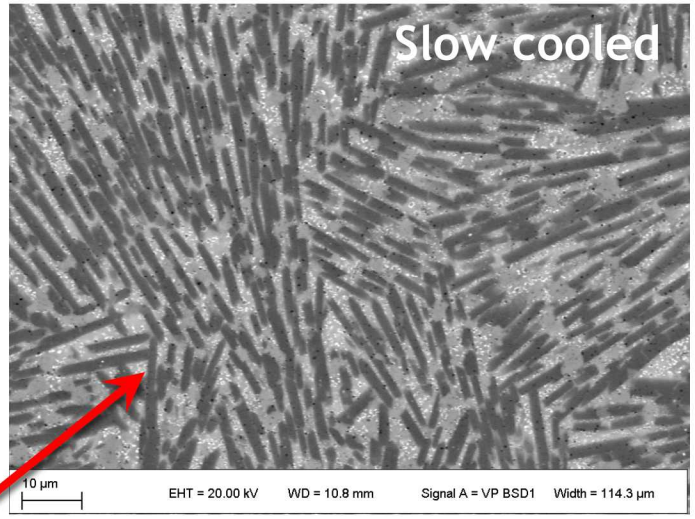

$Li_2Si_2O_5$

Melts ~

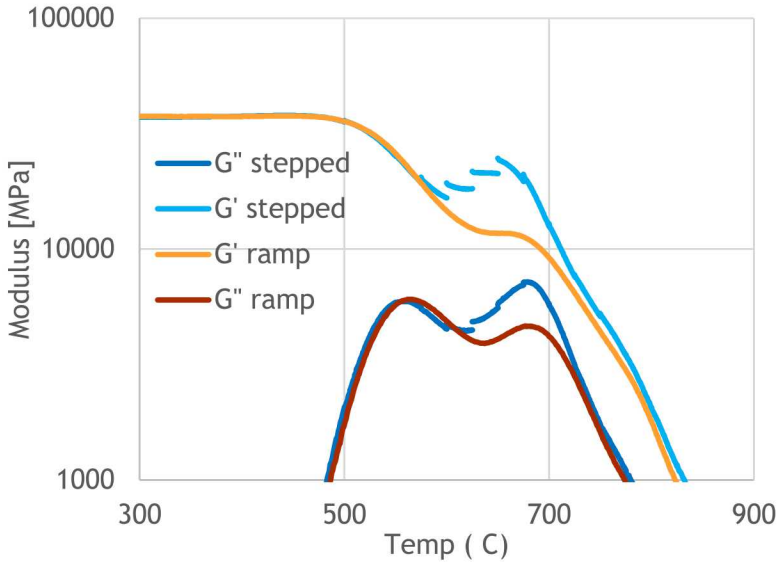

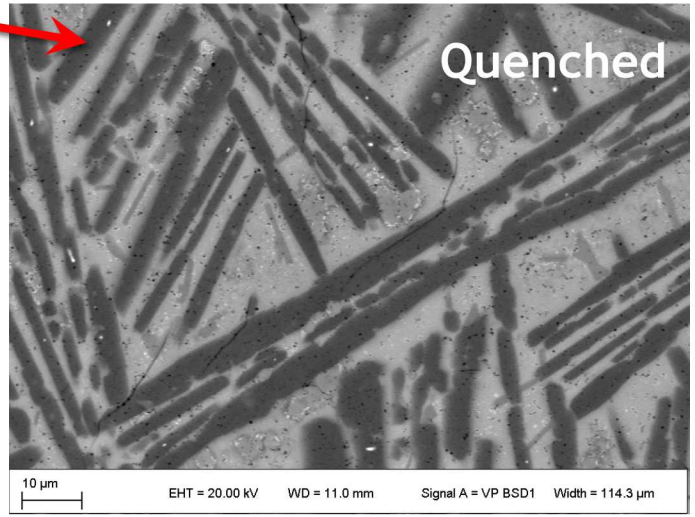

XRD of Crystalline Phases

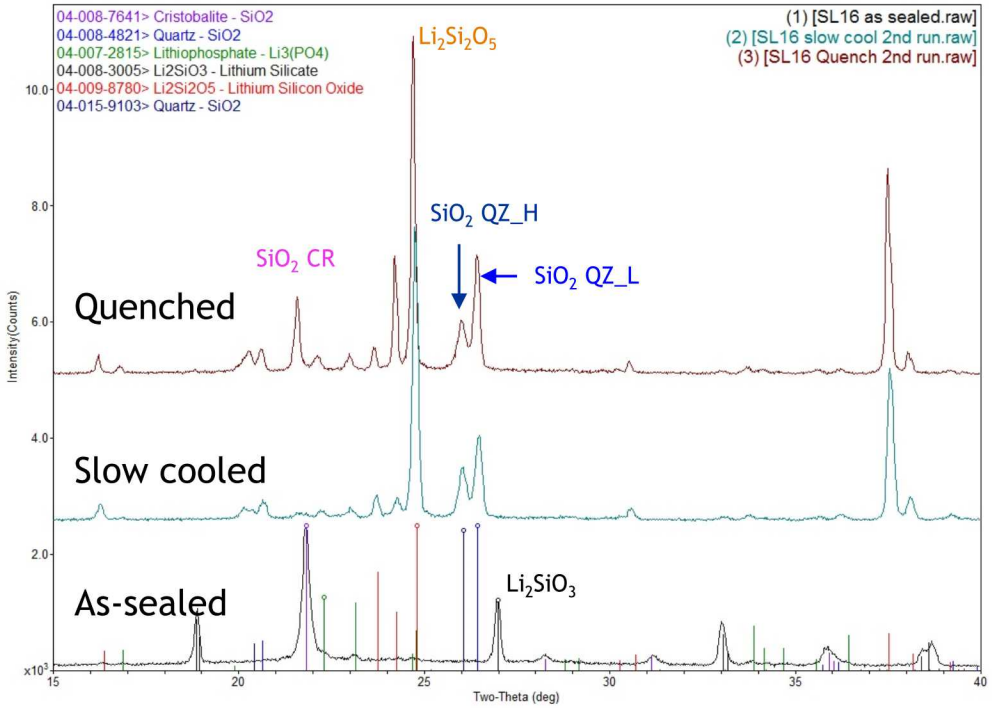

As-sealed

Phase	SL16
	wt%
Quartz Low SiO_2	2.51
Cristobalite SiO_2	24.37
Li_2SiO_3	36.82
Li_3PO_4	7.94
Amorphous	28.36

Quenched

Complete transition
$Li_2SiO_3+SiO_{2CR} \rightarrow Li_2Si_2O_5$

Partial transition
$SiO_{2CR} \rightarrow SiO_{2QZ\_low} + SiO_{2QZ\_high}$

Slow cooled

Complete transition
$Li_2SiO_3+SiO_{2CR} \rightarrow Li_2Si_2O_5$

$SiO_{2CR} \rightarrow SiO_{2QZ\_low} + SiO_{2QZ\_high}$

Cooling from 900 °C, the crystalline phases of glass-ceramics changed from the original as-sealed state

The phase conversion also depended on the cooling rate

Phase conversion likely dominated by bulk diffusion processes in a "viscous" glassy state above glass transition temperature

Thermal Strain Measurement

Rheometers aren't designed to measure thermal expansion coefficients, but they capture the qualitative trends and are able to access a wider range of temperatures

- Magnitude of thermal strain is wrong, perhaps due to inappropriate thermal gap correction calibration.

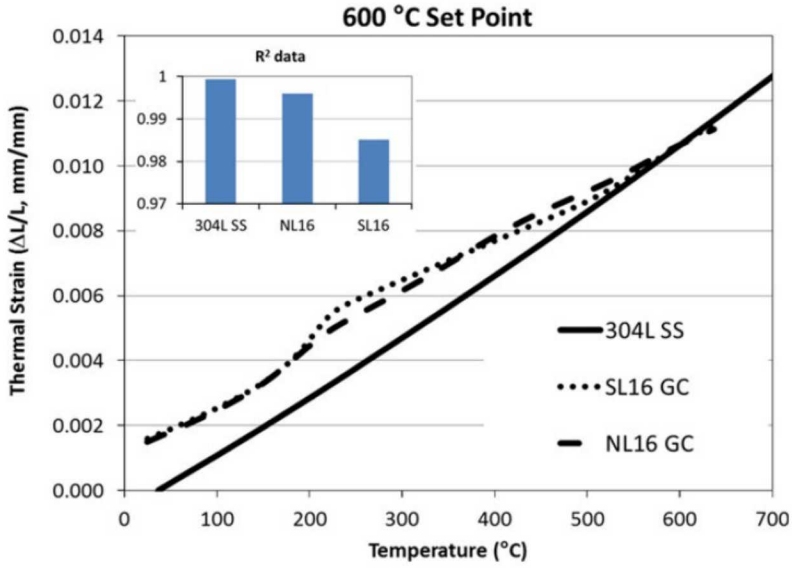

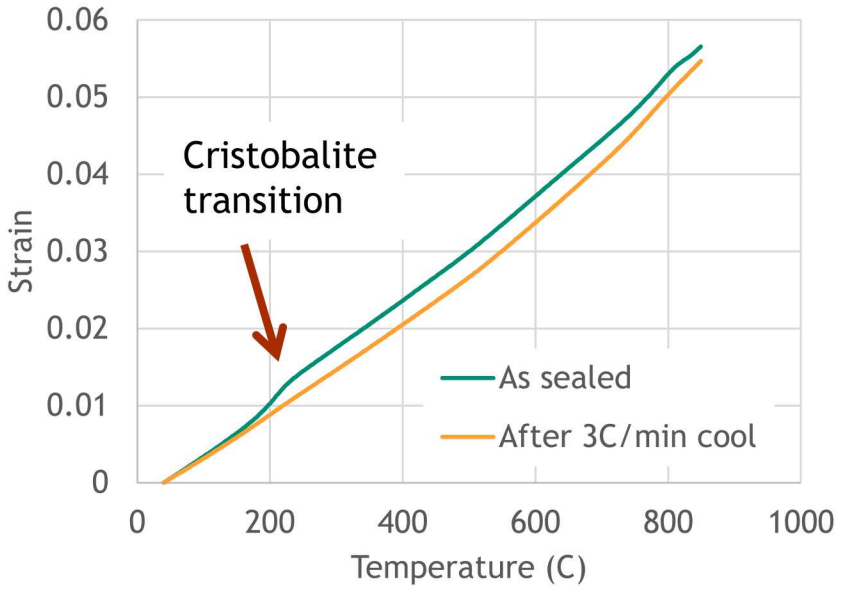

Conclusions

Able to measure shear moduli of glass and glass ceramic sealing materials through their glass transition temperature up to edge of melting transition (-60-950°C)

- Cristobalite alpha-beta phase transition
- Glass transition of material or glassy matrix

Time Temperature Superposition can generate a shear modulus master curve

More complex for glass-ceramics

- Slow-cooled: Acting like a glass with single Arrhenius activation energy related to the glass relaxation
- Quenched: Two distinct Arrhenius activation energies,
  - low temperature dynamics match the relaxation of slow cooled – due to melting of the glassy phase
  - higher temperature dynamics related to the "re-arrangement" of the crystalline phase, or "configurational" relaxation

The role of polymer composite binder on performance of lithium ion batteries


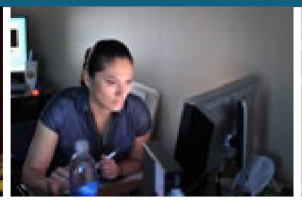
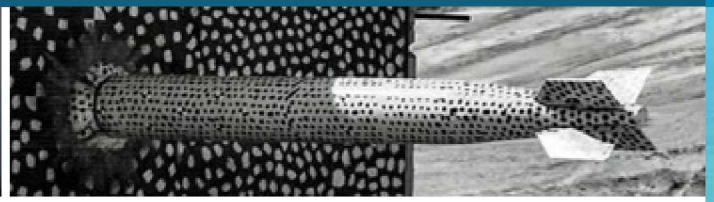

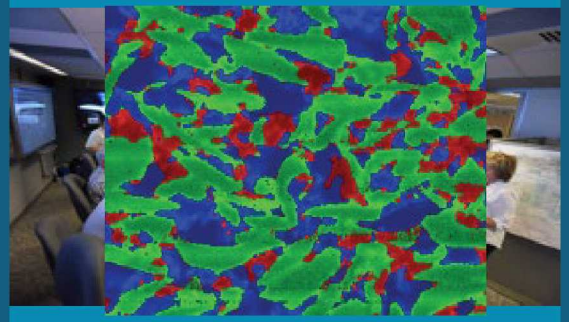

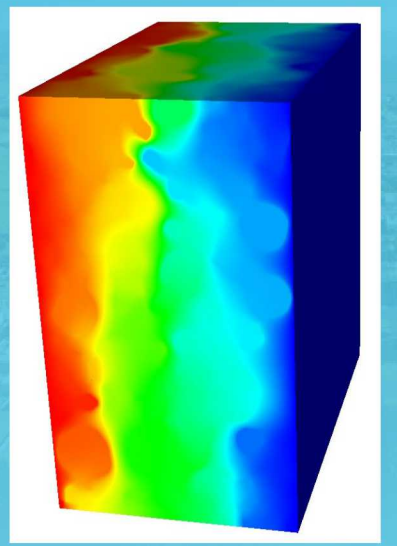

PRESENTED BY
T. Humplik, E.K. Stirrup, A.M. Grillet, S.A. Roberts, B Trembacki & C.A. Apblett

Shaqfeh Symposium 8/12/2019

Sandia National Laboratories is a multimission laboratory managed and operated by National Technology and Engineering Solutions of Sandia LLC, a wholly owned subsidiary of Honeywell International Inc. for the U.S. Department of Energy's National Nuclear Security Administration under contract DE-NA0003525.

Battery Introduction

Batteries convert stored chemical energy into electrical energy

- Lithium is stored in the anode at high chemical potential
- Battery electrodes are particle composites which form bicontinuous percolated network

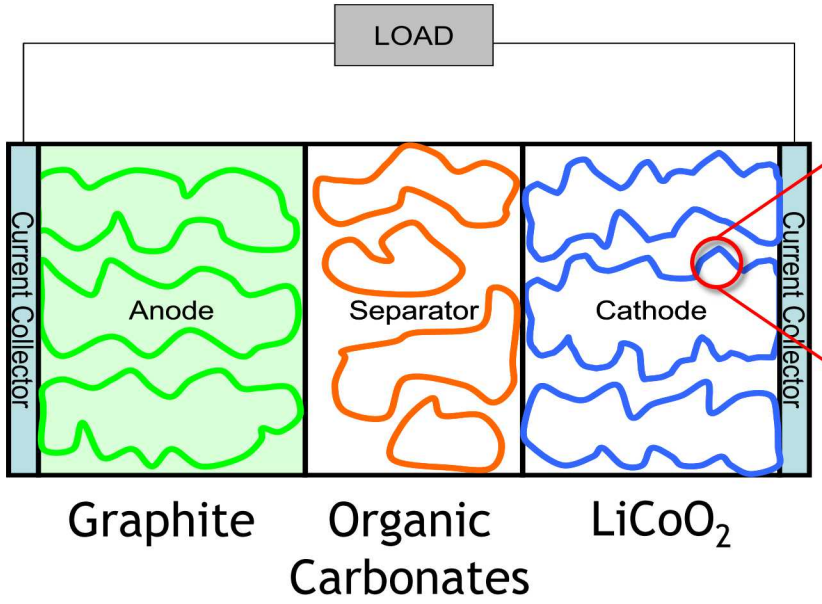

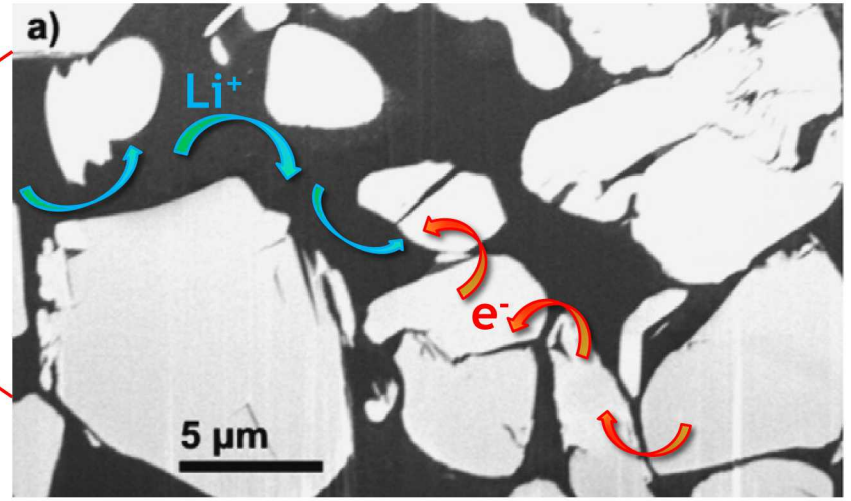

Actual voltage depends on how efficiently lithium ions and electrons are transported

Wilson *et al.* (2011)

Batteries are actually complex composites

Electrode active material particles are held together by binder

- Binder is a mixture of polyvinylidene fluoride (PVDF) and carbon black
- Electronic Conductivity : Binder ~ graphite >> $LiCoO_2$, NMC

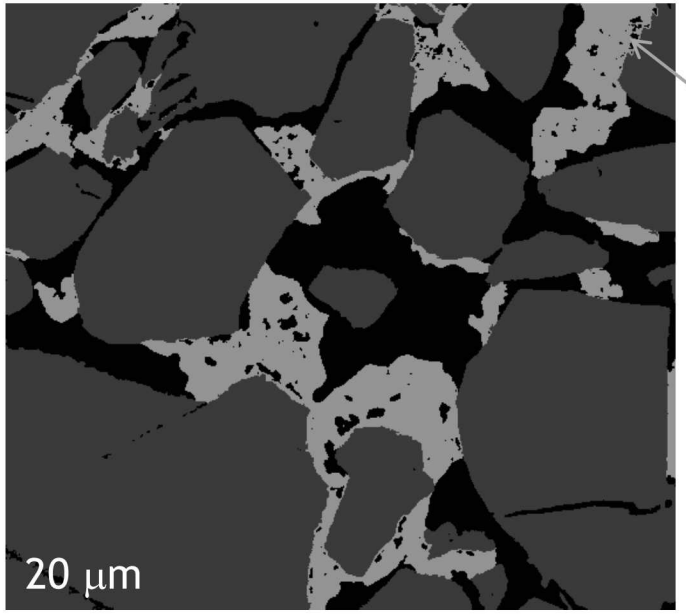

binder

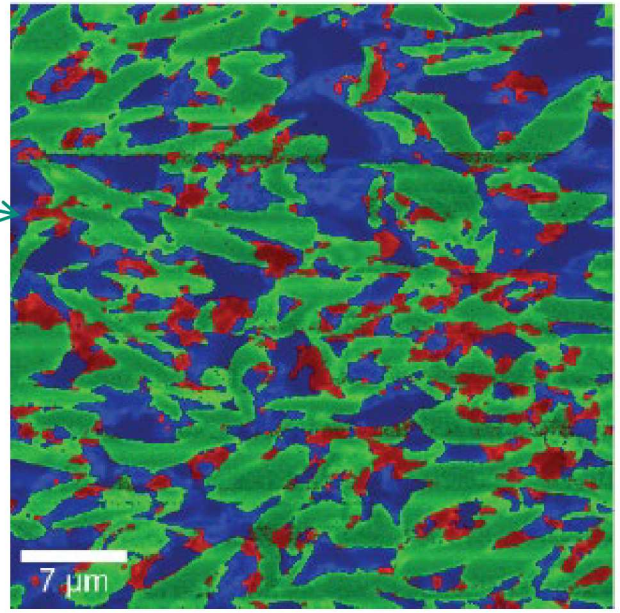

Cathode	94wt% $LiCoO_2$ 3wt% PVDF 3wt% CB **void**
Anode	94wt% graphite 4wt% PVDF 2wt% CB void

Hutzenlaub *et al.* (2012), Doyle et al (2003), Liu et al. (2012); Thomas Beechem (SNL)

Both electrodes swell during charging

Constrained battery pouch cell experiments by Cannarella & Arnold

- See large changes in stress during cycling as cathode and anode swell during charge and shrink during discharge
- Electrodes want to swell after repeated cycling resulting in increased stresses with time

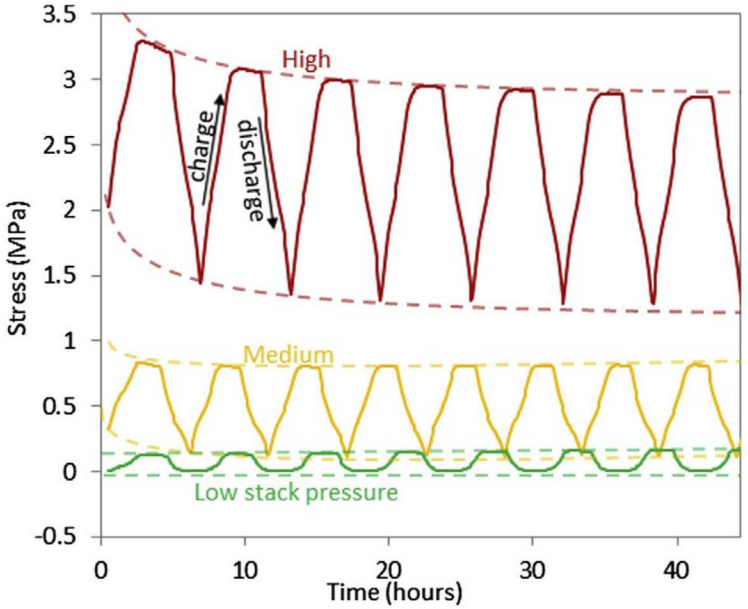

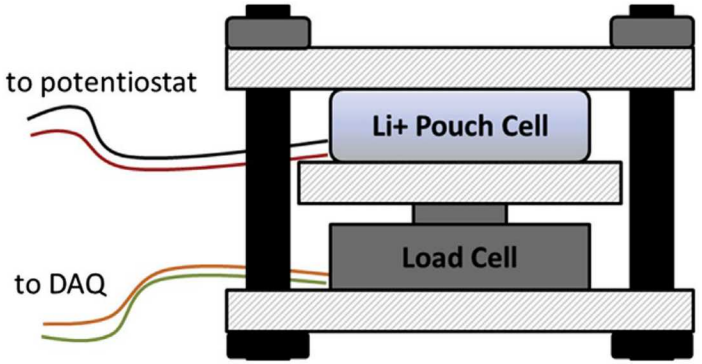

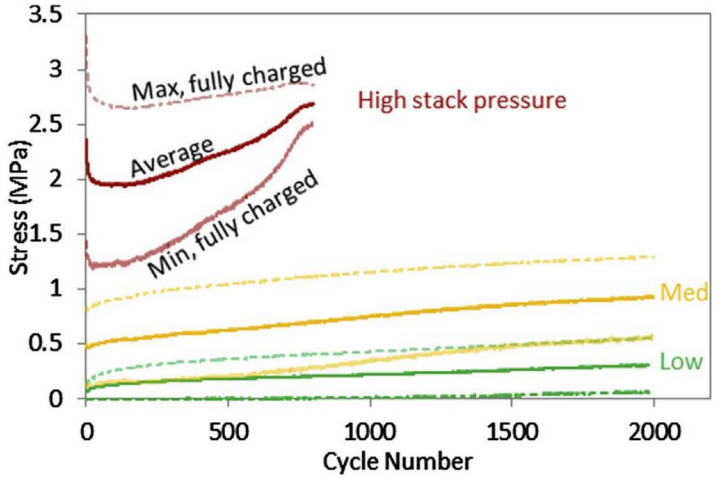

J. Cannarella, C.B. Arnold / Journal of Power Sources 245 (2014) 745e751

Understanding the Role of the Binder

Mechanical

- Mitigating stresses of swelling/ contracting active materials
- Maintaining adhesion of active materials to conductive network

Electrical

- Provide pathway for electron transfer through electrodes
- Decrease resistance (*i.e.*, loss) for cathode

Outline

Battery electrode binders play an important role both mechanically & electrochemically

Mechanical characterization

- Binder has significant impact on stress development within cathode

New coupled mechano-electrochemical characterization

- Under quasi static loads
- Degradation after cycling

Mechanical cycling of binder causes increased internal resistance which degrades battery performance

Morphology of PVDF/Carbon Black Composites

20wt% Carbon Black

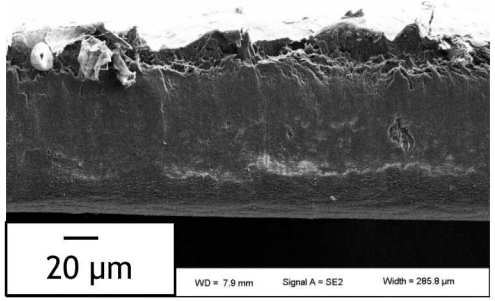

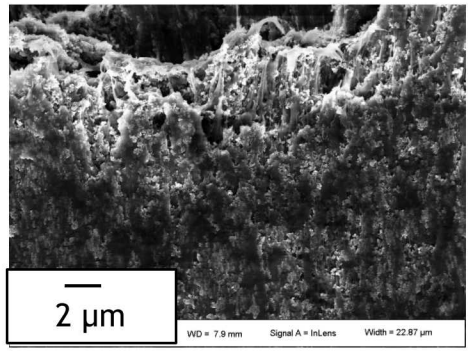

40wt% Carbon Black

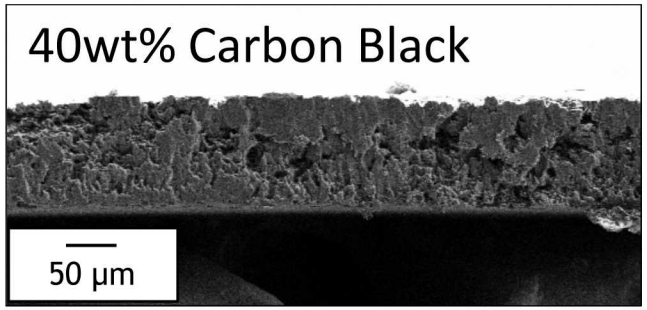

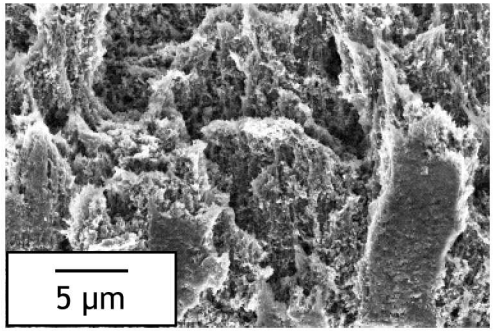

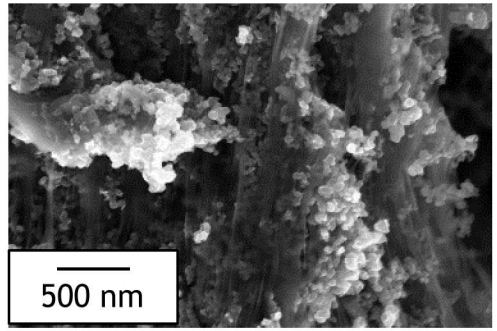

e⁻ paths

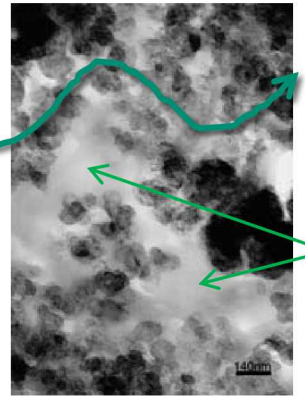

TEM of 33wt% CB in PVDF

Free PVDF

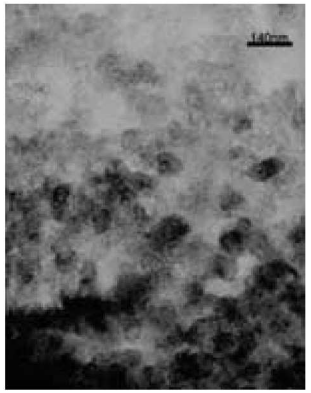

TEM of 45wt% CB in PVDF

No free PVDF

TEM's from Liu *et al.* (2012)

Binder Conductivity in Literature

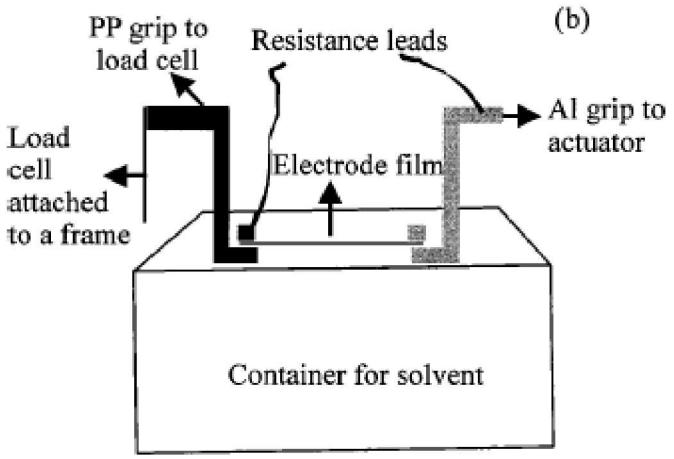

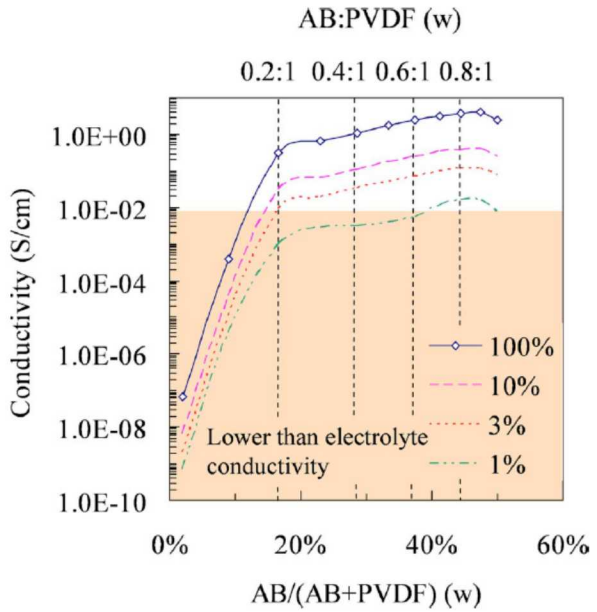

Chen *et al.*[1] investigated the change in resistance of various PVDF/carbon composites (both wet and dry) and during initial cycling in tension

- Small changes in resistivity with ~5 cycles number

Liu *et al.*[2,3] investigated the effect of varying carbon concentration on film conductivity

- Substantial characterization of binder morphology, organization with varying CB concentration

They both used 4 point probe technique to calculate conductivity

- We are using oscillatory method
- Measure different conductivities

1. Chen et al. (2003) 2. Liu et al. (2012) 3. Liu et al. (2008)

Rheometer/Impedance Measuring System

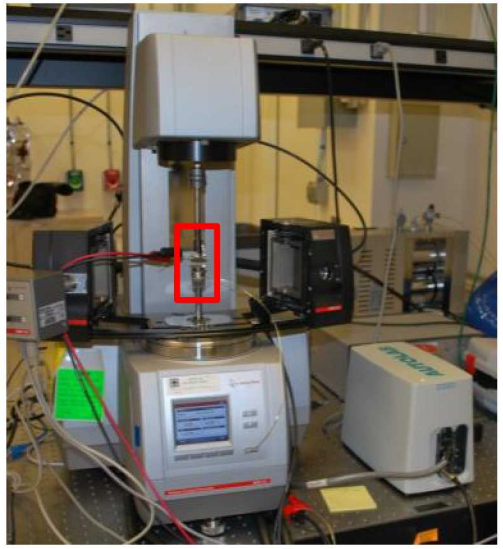

Measure electrical properties of system during rheological tests

- Anton Paar MCR 502 rheometer
  - Compression of binder disks
- Metrohm PGASTAT204/FRA 32
  - Potentiostat/galvanostat 10 μHz - 1 MHz
  - Welded wire leads to plates to reduce lead resistance
  - Performing Electrical Impendence Spectroscopy

Qualified that combined tool can measure a variety of electrochemical systems

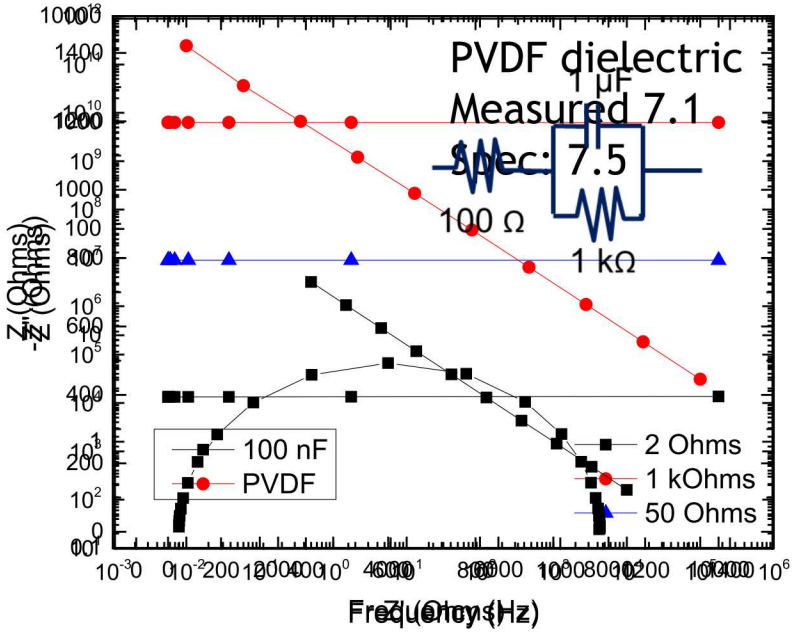

Mechanical Cycling of Dry Binder Film

PVDF/CB composite (30wt% CB)
(6x 5 mm diameter discs, ~500 µm thick)

Procedure:
28 kPa – 2.8 MPa – 28 kPa at ~4C cycle rate

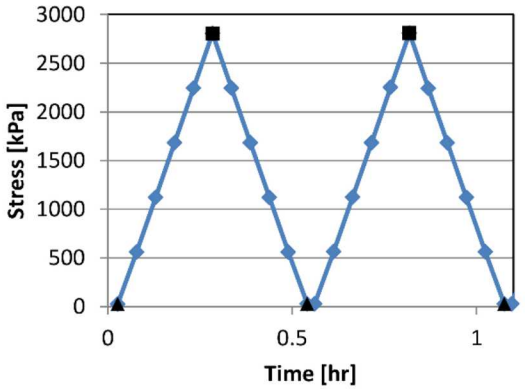

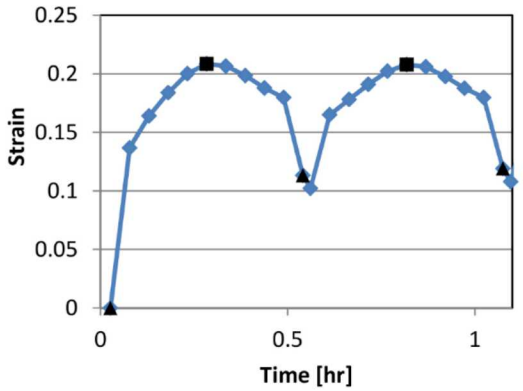

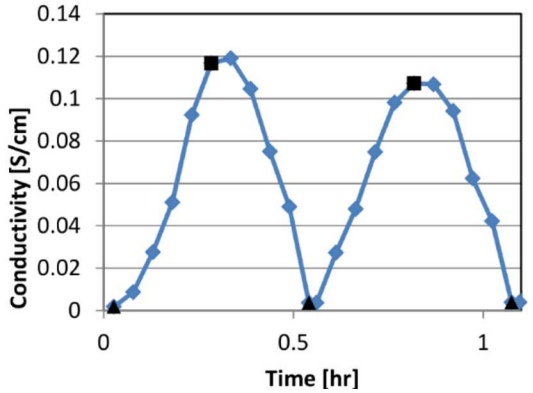

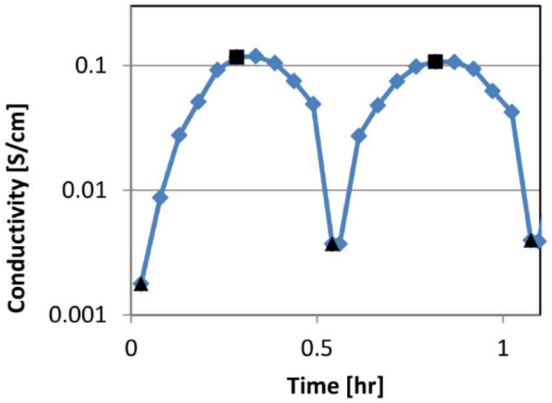

Plastic deformation after first cycle (flattening of disks or surface non-uniformities)

Exhibit strong dependence of applied load (and resulting strain) on conductivity of film

- Changes by two orders of magnitude

Mechanical Cycling of Dry Binder Film

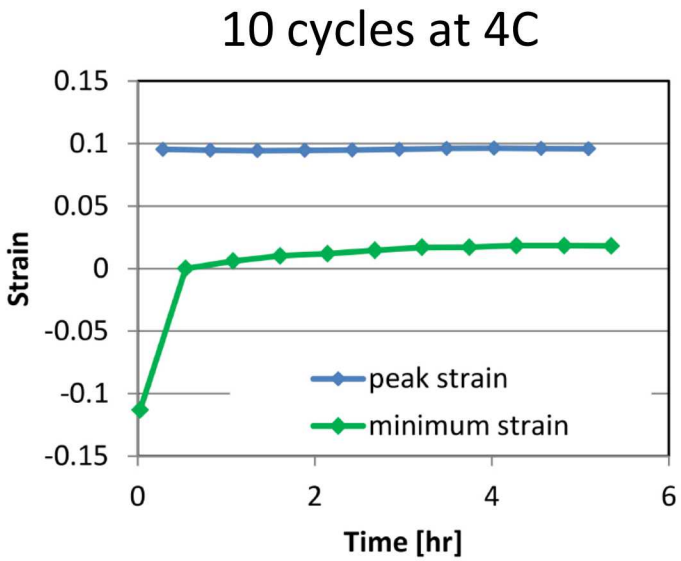

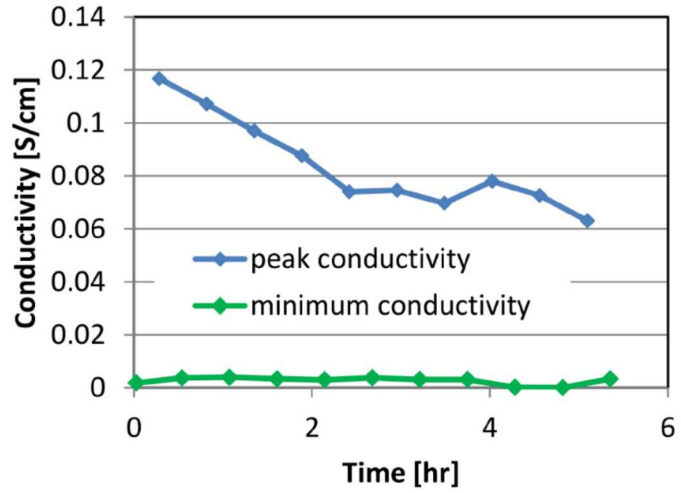

Mechanical cycling

- 27 kPa – 2.8 MPa – 27 kPa
- 4C (cycle ≈ 32 min)
- 10 cycles (5+ hours)

Slow consolidation of binder film

Significant 30% decrease in binder electrical conductivity after 10 cycles

- SEM imaging of binder films before and after cycling show no obvious morphology changes (cracks, delamination from the particles, etc.)

Mechanical Cycling of Dry Binder Film

Accelerated cycling

10 cycles at 120C between each measurement cycle at 4C

- 28 kPa – 2.8 MPa – 28 kPa
- 4C (cycle ≈ 32 min), 10x 120C (cycle ≈ 1min)
- 266 total cycles (19 hours)

30wt% Carbon black dry binder film

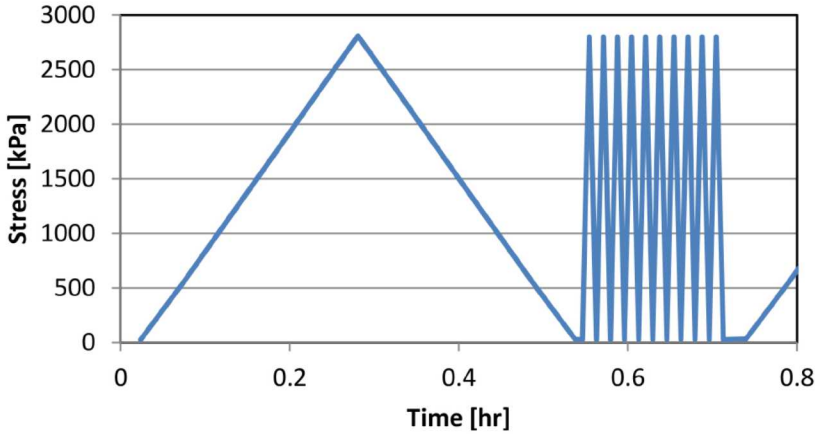

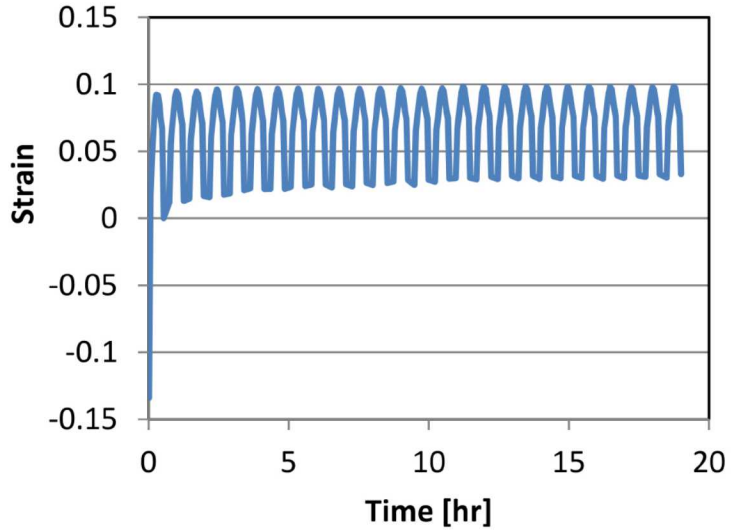

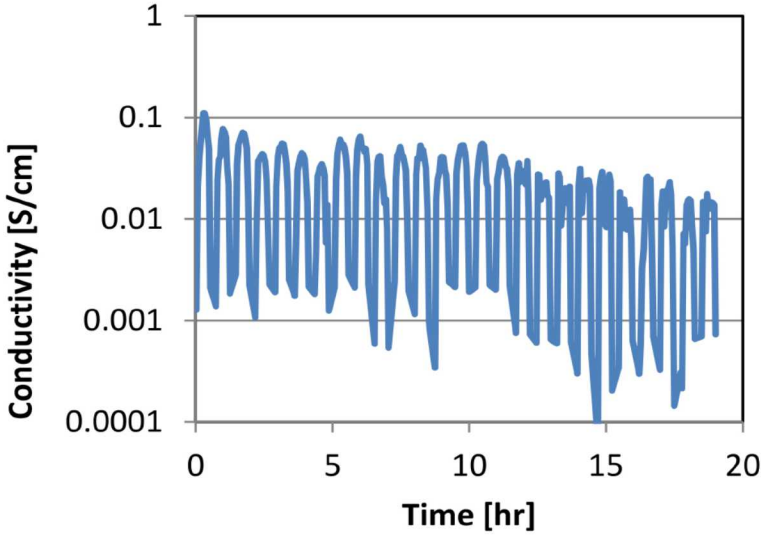

Mechanical Cycling of Swollen Binder Film

Examined affect of carbon black concentration

Binder absorbs 20-40wt% of propylene carbonate (PC) solvent

Cycled using same accelerated cycling protocol

- 4C (cycle ≈ 32 min), 10x 120C (cycle ≈ 1 min)

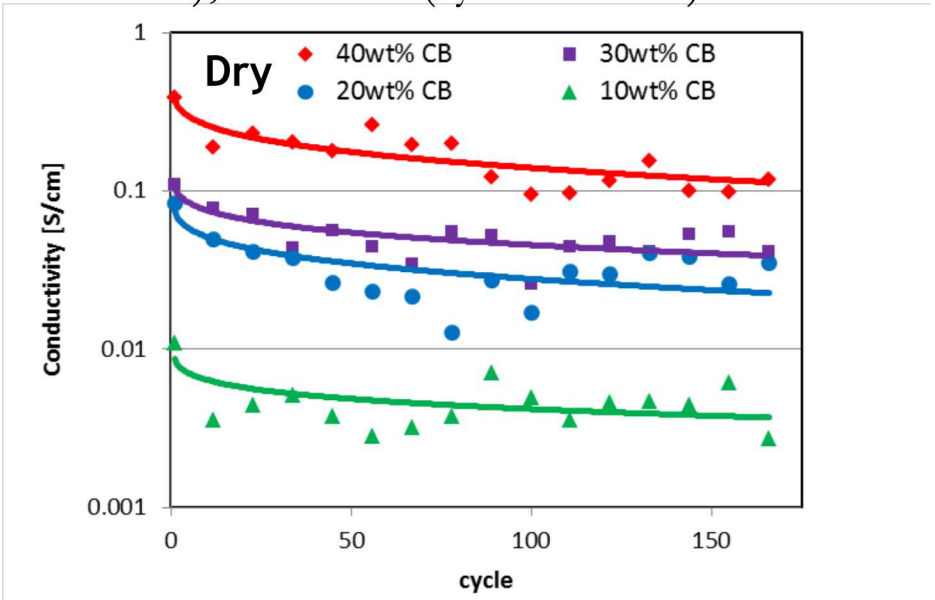

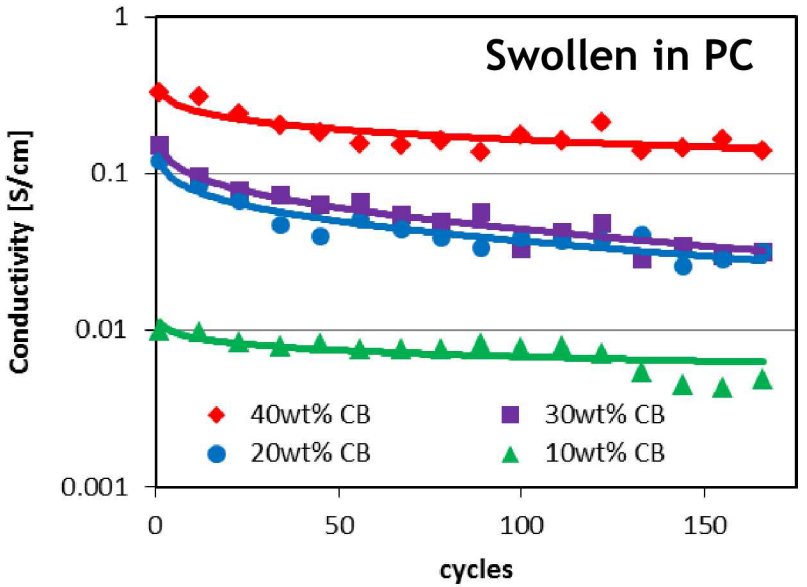

- Significant decrease in binder conductivity as a function of mechanical cycling between 45-75%
- Same for both Solvay 5130 and Kureha W #1300 battery grade PVDF polymers

Mechanical Cycling of $LiCoO_2$ Cathode

Cathode depends on the binder for reducing internal resistance

- Active material: $\sigma_{LiCoO2}=10^{-6}$ S/cm vs 0.5-0.05 S/cm for binder
- Propylene carbonate solvent: $\sigma_{PC}=10^{-10}$ S/cm

Similar trend in degradation of electronic conductivity of cathode

- Binder conductivity changes could drive degraded battery performance

94wt% $LiCoO_2$
6wt% PVDF/CB
solvent

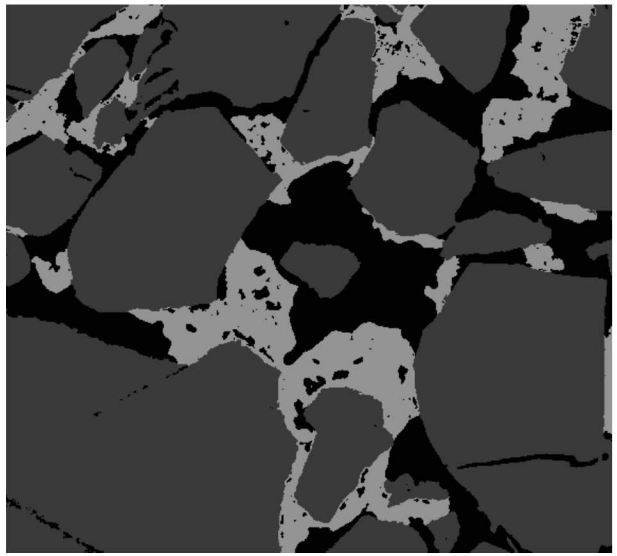

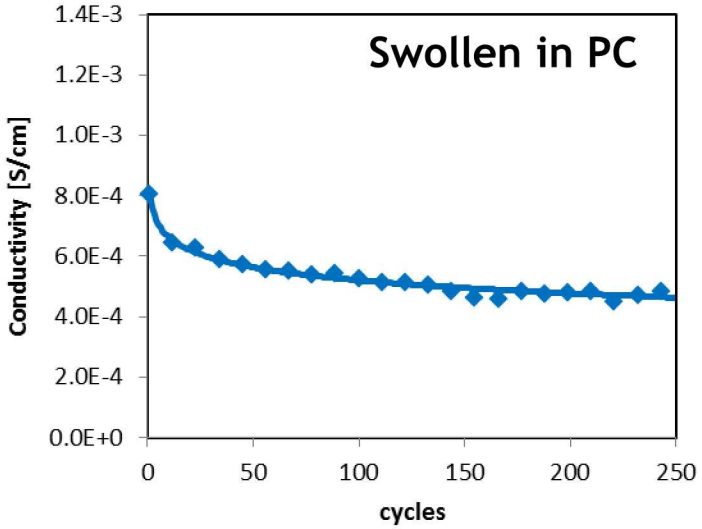

Hutzenlaub et al. (2012), Nishizawa et al. (1998)

Mesoscale Simulation of Electrical Conduction

Higher resolution particle data set for NMC cathode

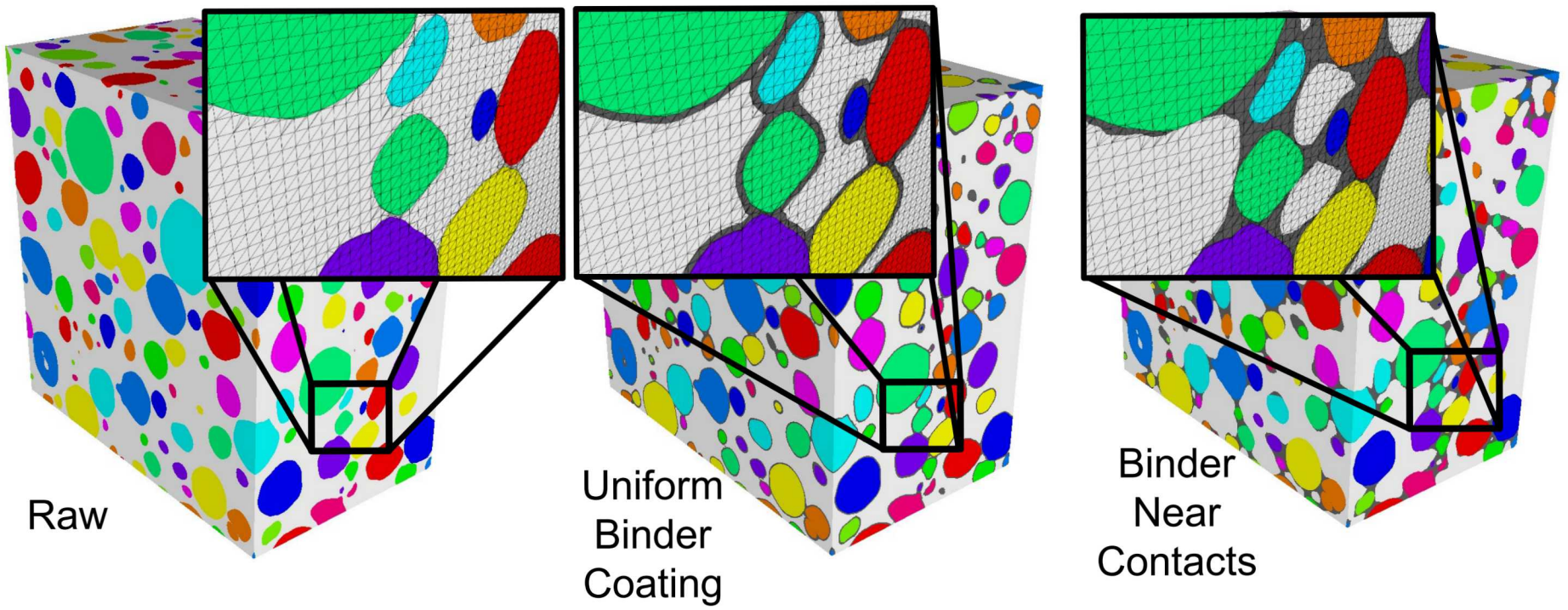

Trembacki *et al* (2017)

Binder key for electrical conduction

NMC conductivity also much lower than binder

Electron flux

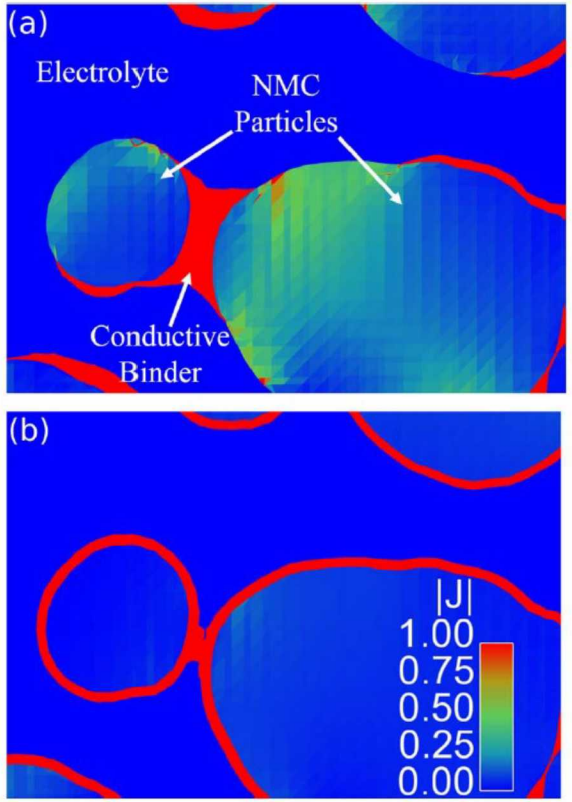

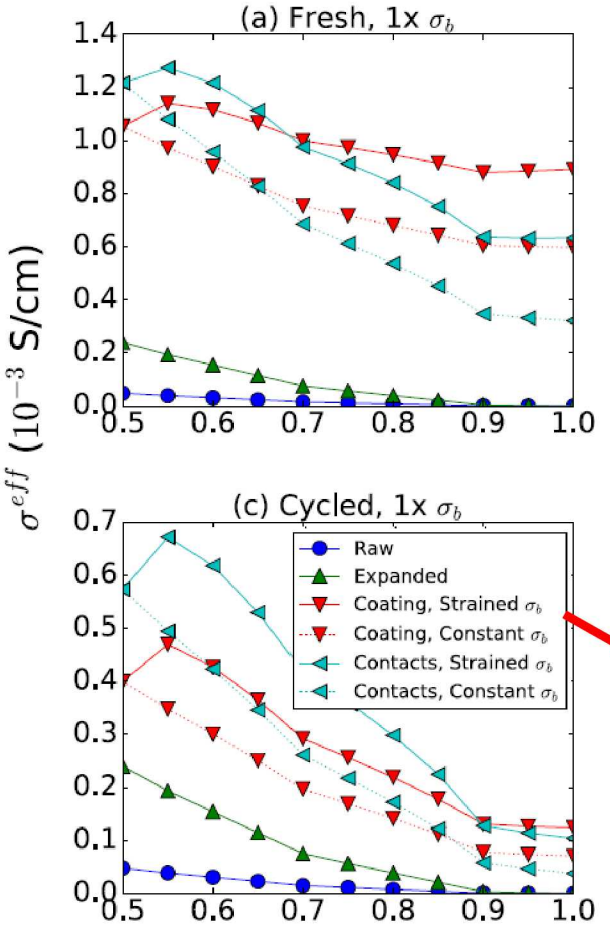

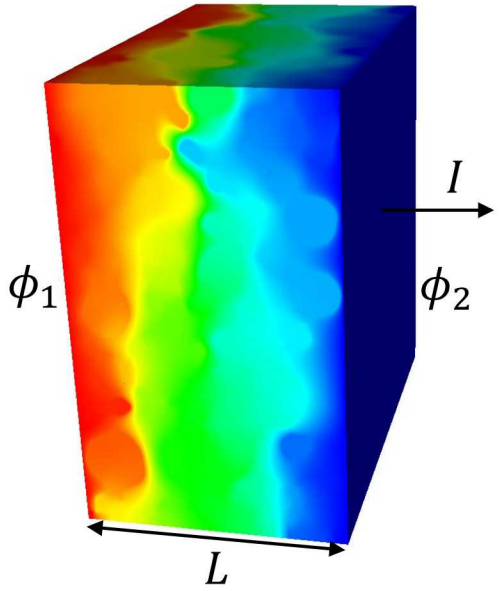

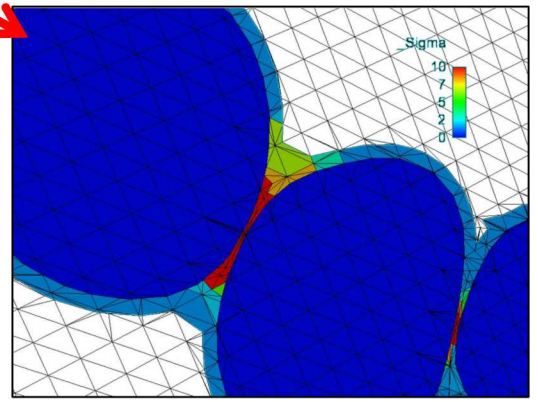

Trembacki *et al* (2017)

Conclusions and Future Work

Mechanical properties

- Binders are generally elastic solids
  - Dry: E= 2GPa, Wet: E=200 MPa
  - Properties of composites do not depend on carbon concentration
- Binder has a large impact on stress generated during charging

Electrical properties

- Conductivity of both the binder and full cathode is strongly dependent on the applied stress/strain conditions
- Conductivity of the binder and cathode both decrease significantly with mechanical cycling

Future work:

- Cycling behavior of wet binder and cathode
- Active work on modeling stress development in electrodes

This work was funded as part of Sandia's Laboratory Directed Research and Development Program.

LDRD
LABORATORY DIRECTED RESEARCH & DEVELOPMENT

Synthesis of PVDF/CB Binder films

Solvay 5130 PVDF

Denka Carbon Black

Film thickness on the order of 100 - 200 μm

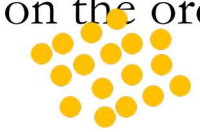

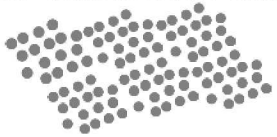

Dissolve in N-Methyl-Pyrrolidone T=50-70°C

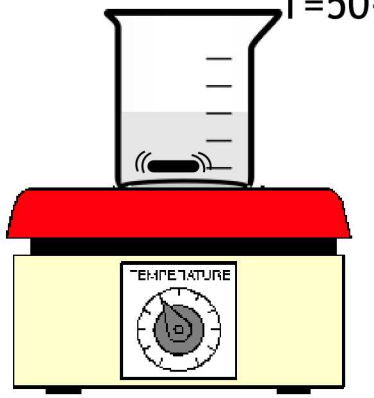

Mix into solution 1800RPM 2hrs

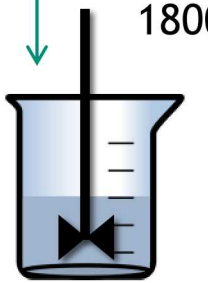

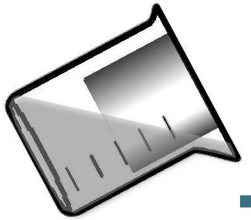

Pour onto Si wafer

Dry in vacuum oven at 110°C for 12 hours

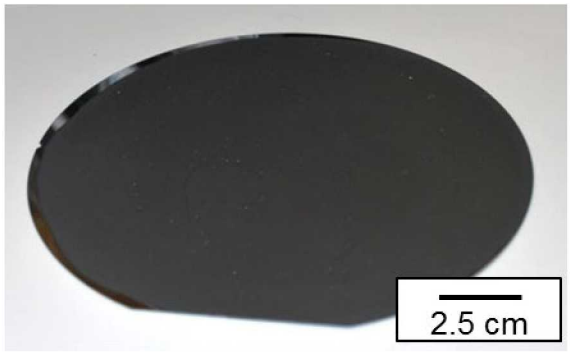

Mechanical Testing - DMA

Netzsch
- Probe
- Probe

Mechanical Properties – Dry Binder

Storage modulus >> Loss modulus for entire temperature range

Binder softens at higher temperature

Despite large differences in morphology, no dependence on carbon black concentration

Elastic modulus for dry binder ranges between 1.5 – 2.25 GPa

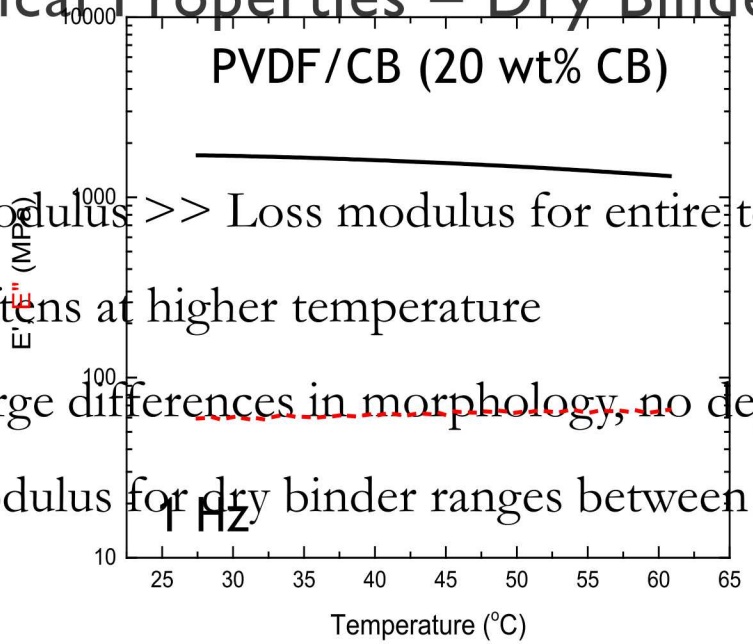

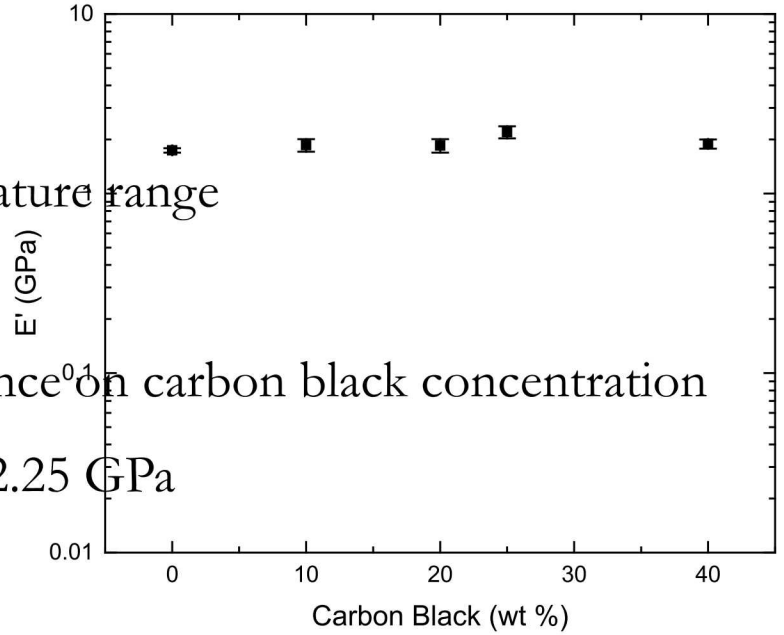

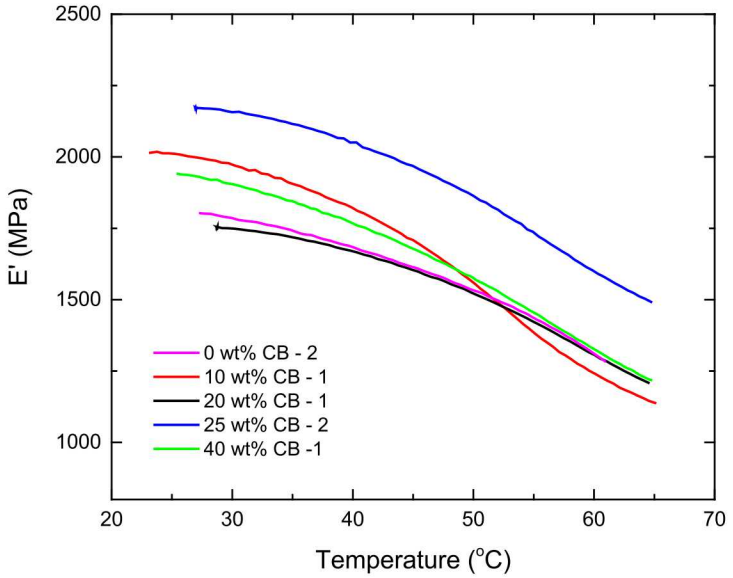

Electrolyte Swollen (Wet) Binder Properties

Immersed binder samples within propylene carbonate (PC) for at least 24 hours

- Samples absorb between 25 – 35 wt% in propylene carbonate within 6 hours of immersion

Decreased moduli (≈ 200 MPa for wet compared to ≈ 2 GPa for dry)

No clear trend as a function of carbon black weight percent

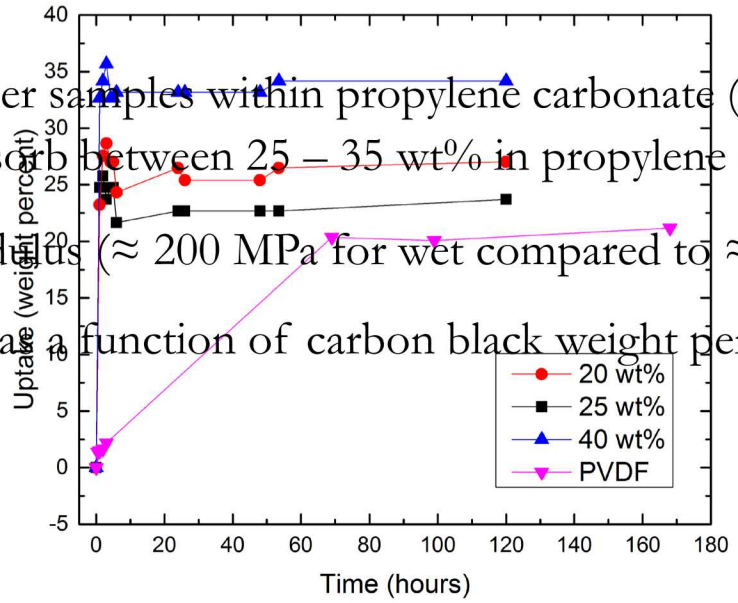

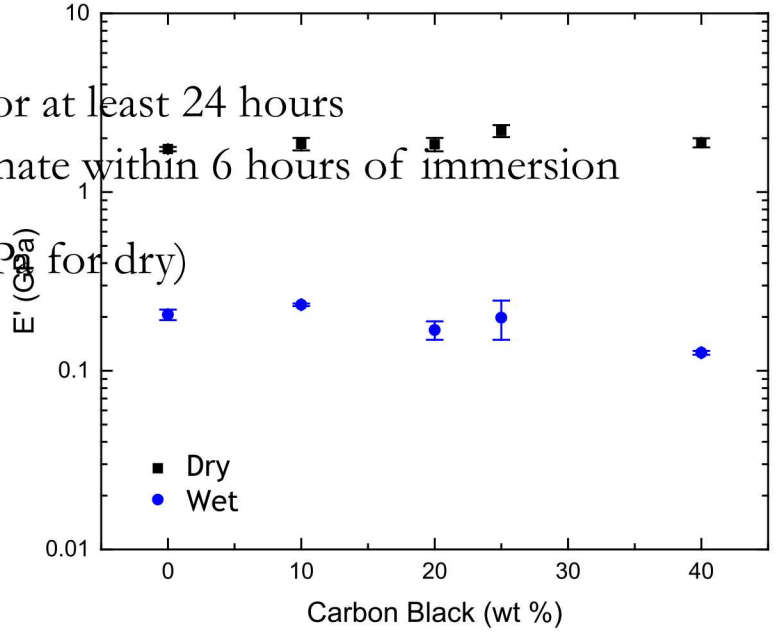

Reconstruction of Cathode Microstructures

Reconstructi Avizo fron slices at s

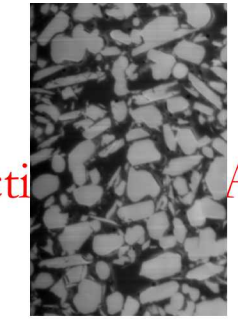

FIB/SEM/EDS images of $LiCoO_2$ cathode

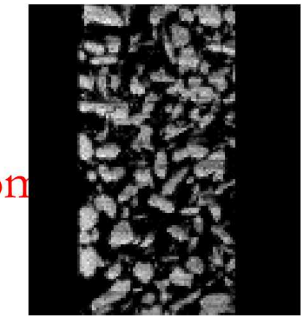

Multivariate principal component analysis

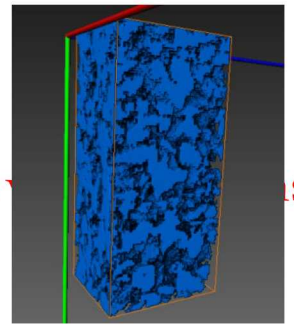

Binary mode recreated from images

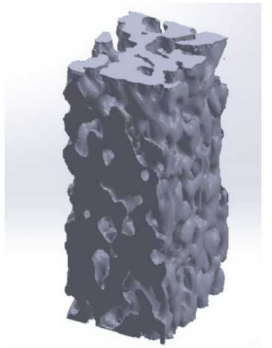

Surface mesh from binary model

Conformal De EM (CI nethoc

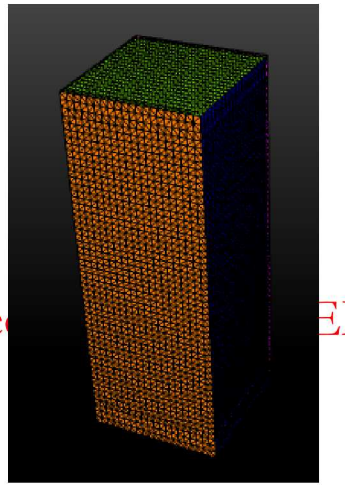

Background 3D mesh

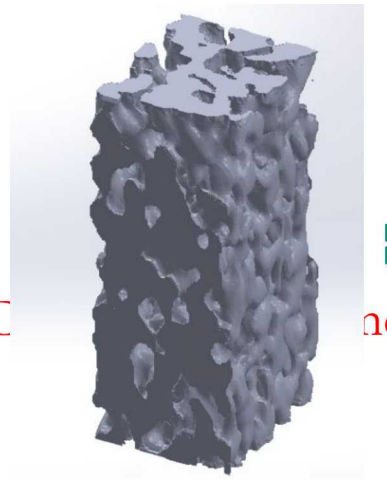

Cathode surface mesh (STL)

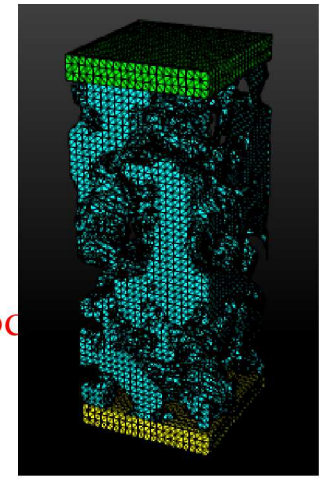

3D Mesh superimposed on cathode particles

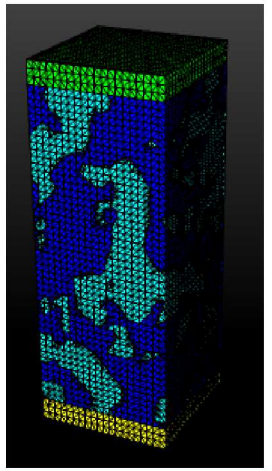

3D Mesh superimposed on cathode particles and electrolyte

Roberts et al (2014); Noble (2010); Mendoza et al., Electrochimica Acta (submitted)

Importance of Binder in Cathode Mechanics

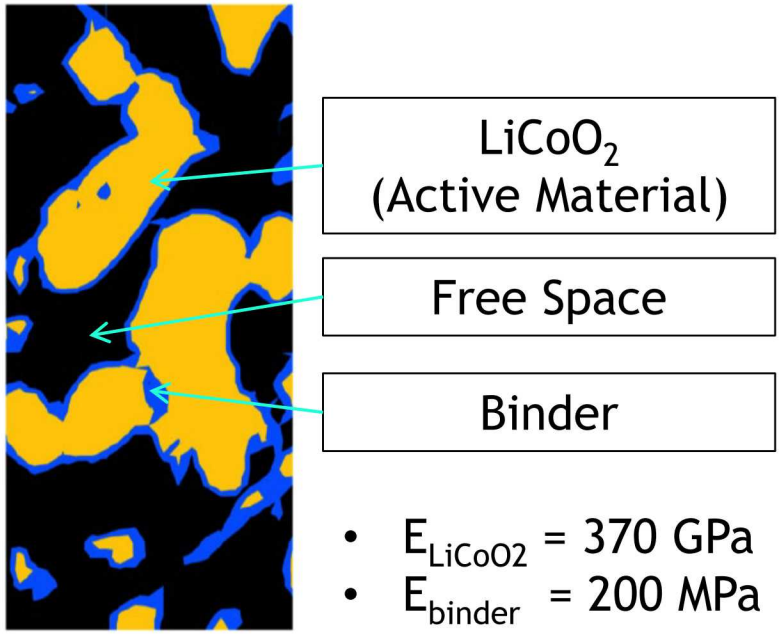

- E_{LiCoO2} = 370 GPa
- E_{binder} = 200 MPa

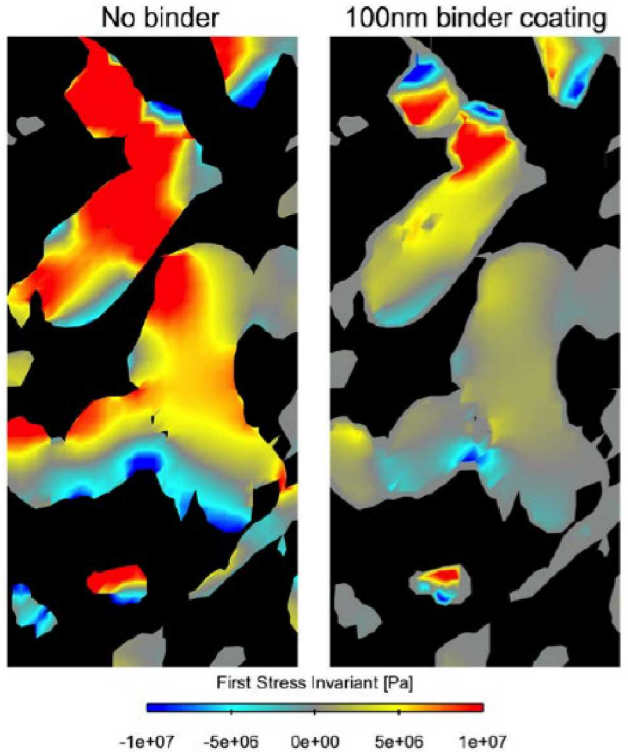

- Calculate the stress and effective modulus in the cathode due to an imposed tension strain
- Inclusion of polymeric binder (100 nm thickness) uniformly covering active material decreased maximum observed stress by 50 %

Mendoza et al., Electrochimica Acta (submitted), Malave 2014

Cycling Behavior of Dry Binder Film

PVDF/CB composite (40wt% CB)
(5 mm disc, ~175 μm thick)

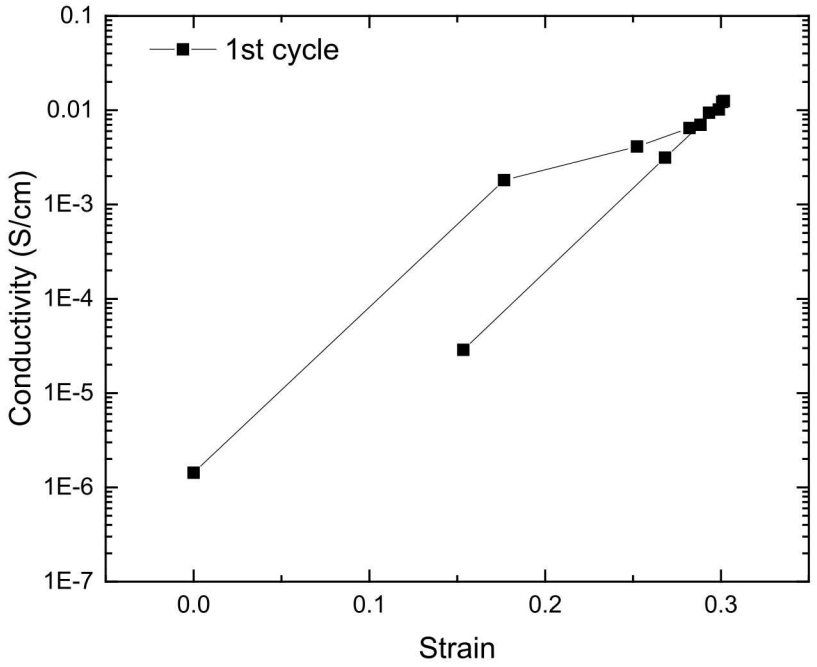

Procedure:
250 kPa – 2.5 MPa – 250 kPa at
5C (24 min total)

Cycled applied stress from ≈ 250 kPa to 2.5 MPa

- Plastic deformation after first cycle (flattening of surface non-uniformities)

Exhibit strong dependence of applied load (and resulting strain) on conductivity of film

- Changes by over four orders of magnitude

Cycling Behavior of Dry Binder Film

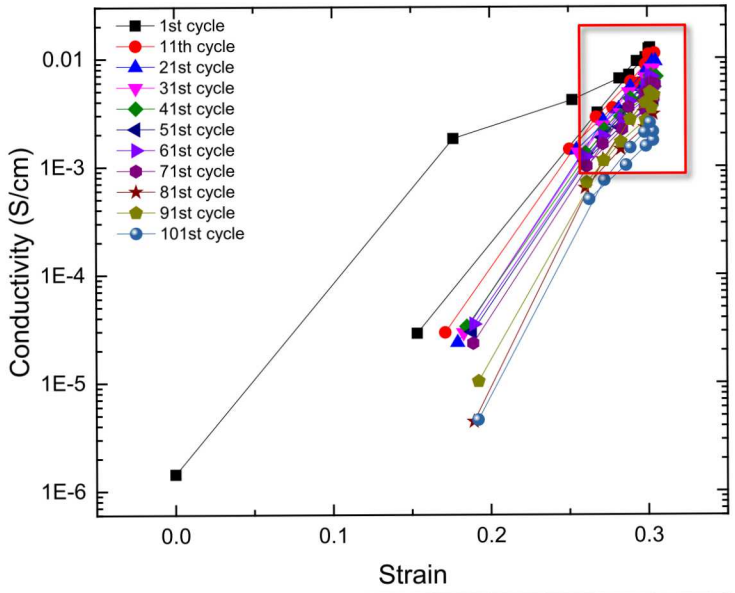

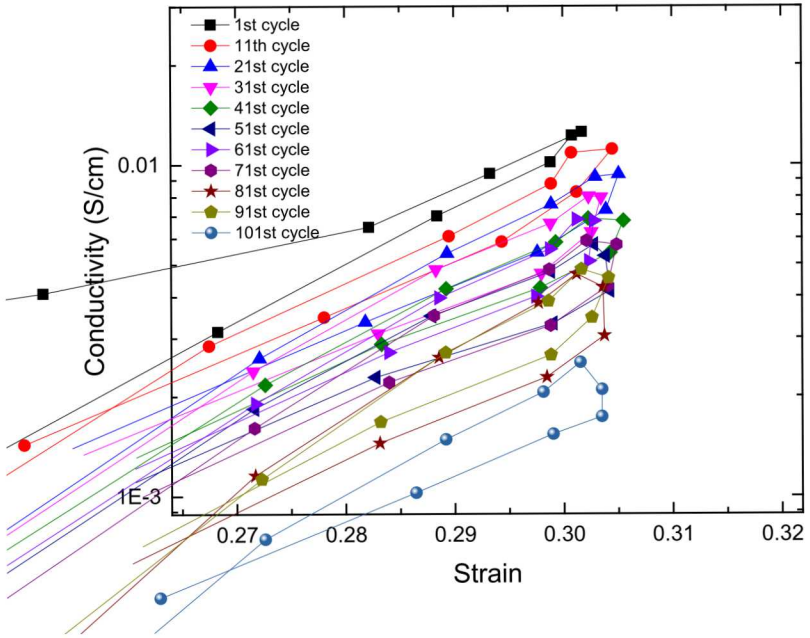

Procedure:

- 250 kPa – 2.5 MPa – 250 kPa
- 5C (cycle ≈ 24 min), 9x 120C (cycle ≈ 1 min)
  - 101 total cycles

Significant decrease in binder conductivity as a function of cycling

- Most secondary batteries can be cycled up to 1000 times during lifetime

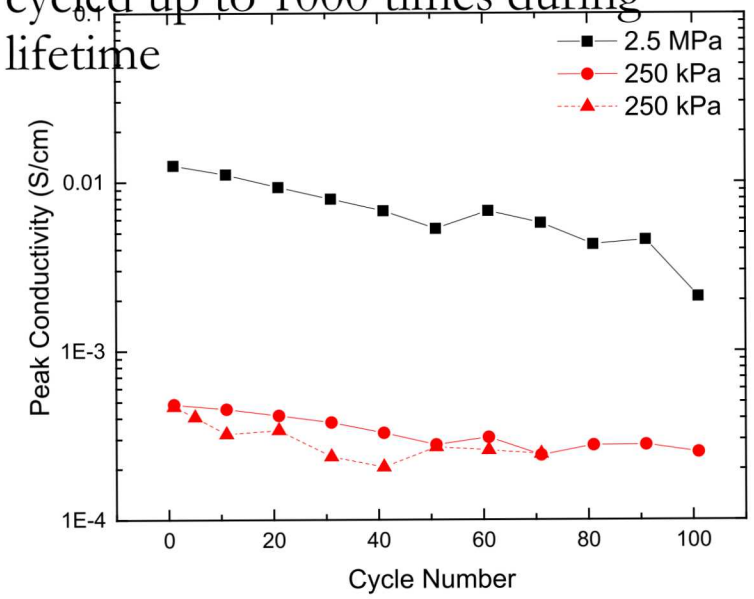

Cycling Behavior of $LiCoO_2$ cathode

Cathode conductivity is much lower than pure binder

- 94 wt% LiCoO2 : 3wt% PVDF : 3wt% Carbon black

Similar trend in degradation of conductivity of cathode

- Binder conductivity changes could drive degraded battery performance

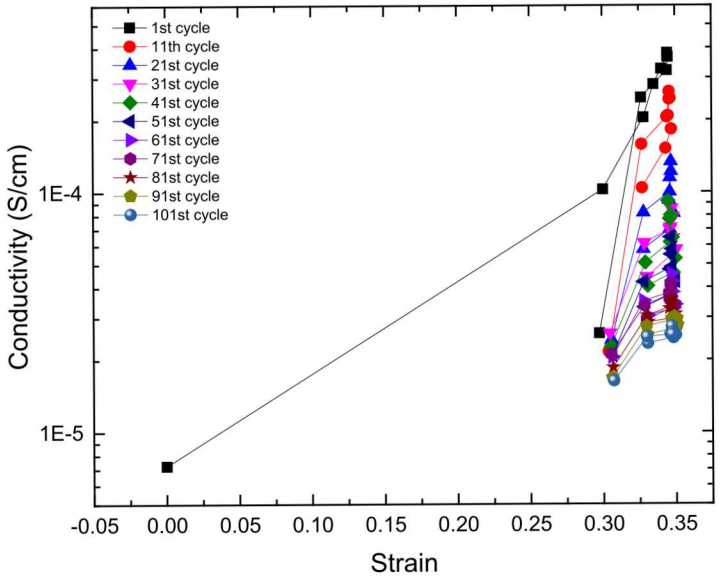

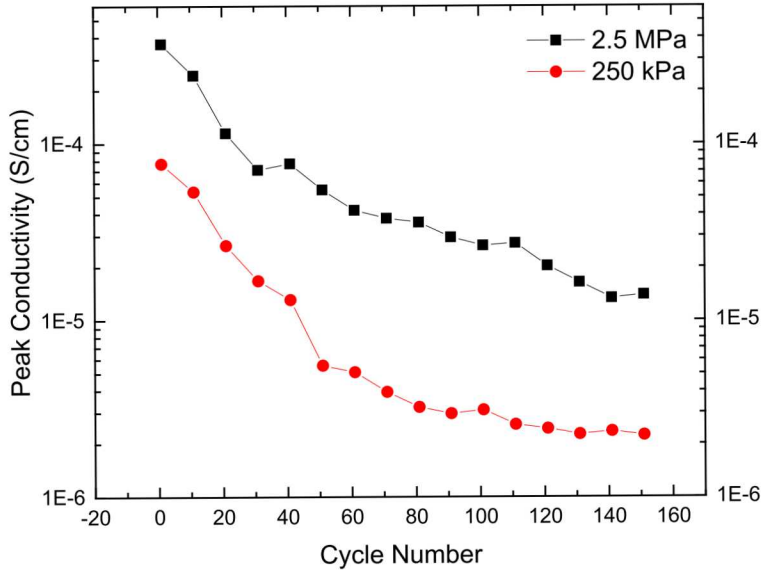

Impact of Binder Conductivity on Cathode

Calculate the effective electrical conductivity of a representative cathode microstructure as the binder conductivity decreases.

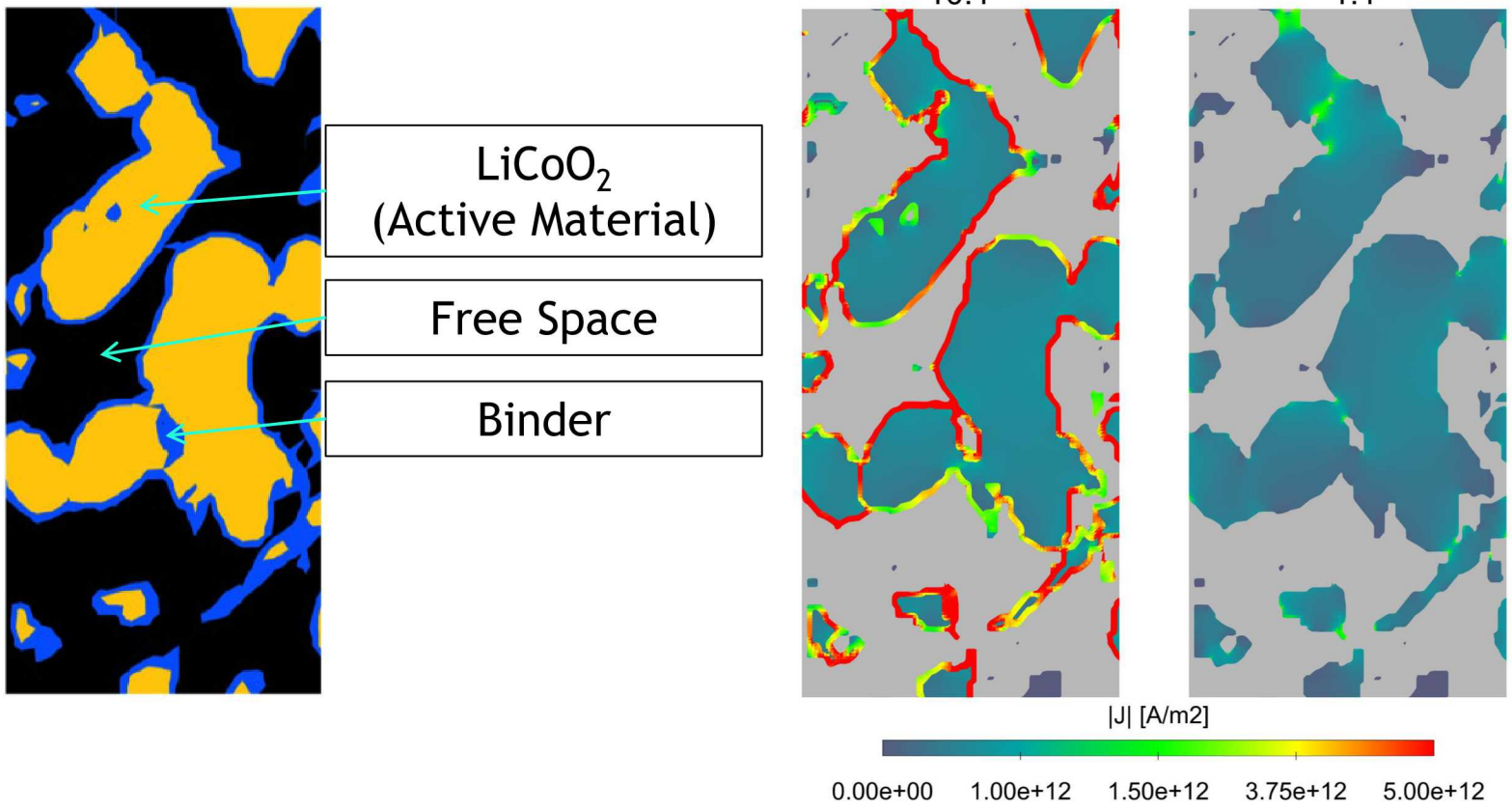

Impact of Binder Conductivity on Cathode

Effective resistance of a cathode is strongly dependent on